UNCLASSIFIED

AD NUMBER
AD820453

LIMITATION CHANGES

TO:

Approved for public release; distribution is unlimited.

FROM:

Distribution authorized to U.S. Gov't. agencies only; Administrative/Operational Use; SEP 1967. Other requests shall be referred to Air Force Office of Scientific Research, Arlington, VA.

AUTHORITY

AFOSR, per ltr dtd 12 Nov 1971

THIS PAGE IS UNCLASSIFIED

AD820453

COMPOSITE SOLID PROPELLANT IGNITION MECHANISMS

AFOSR SCIENTIFIC REPORT

SEPTEMBER 1967

BEST
AVAILABLE COPY

Prepared for

UTC 2139-ASR 2

Qualified requestors may obtain additional
copies from the Defense Documentation Center

COMPOSITE SOLID PROPELLANT
IGNITION MECHANISMS

Research and Advanced Technology Department
UNITED TECHNOLOGY CENTER
Division of United Aircraft Corporation
Sunnyvale, California

AFOSR SCIENTIFIC REPORT

Prepared by

Larry J. Shannon

FOREWORD

ABSTRACT

This report describes the work performed under AFOSR Contract No. AF 49(638)-1557 during the period 1 April 1966 through 31 March 1967. Surface structures of thermoplastic and elastomeric fuels were found to be markedly different upon exposure to conductive heating from a doubly compressed stagnant gas at oxygen concentrations below those required to cause ignition. The thermoplastic polymers exhibited a molten surface, while the elastomeric fuels showed no visible changes. Vaporization followed by a gas-phase reaction is the probable ignition mechanism for the thermoplastic fuels in the shock tube environment. A gas-solid reaction may occur in the ignition of elastomeric polymers. No general conclusion can be drawn regarding the precise nature of the oxygen-polymer ignition process in the shock tube environment as consideration must be given to the physical structure of the polymer surface.

Ignition characteristics of several representative ammonium per-chlorate composite propellants were studied using the arc-imaging furnace. The nature of the fuel component was found to have the major influence on the ignition time, and the effect is related to the initial pressure. A model describing composite propellant ignition in a neutral environment was formulated and programmed for computer studies.

CONTENTS

ILLUSTRATIONS

ILLUSTRATIONS (Continued)

TABLES

ABBREVIATIONS

Al   aluminum

AP   ammonium perchlorate

CTPB   carboxy-terminated polybutadiene

dc   direct current

F   radiant flux

IR   infrared

P   pressure

PBAN   polybutadiene-acrylic acid-acrylonitrile

PIB   polyisobutylene

PU   polyurethane

T_{Ai} autoignition temperature

UTC   United Technology Center

1.0 INTRODUCTION

Solid propellant combustion starts with ignition, and the ignition characteristics of composite solid propellants depend on the simultaneous interaction of many physical and chemical processes. The study of propellant ignition is complicated by the fact that the contribution of individual unit processes may shift with changes in propellant composition, gaseous environment, heating mode and rate, and pressure. The magnitude of the ignition time and its dependence on measurable independent variables provide the principal clues for the determination of the significant processes.

This research program encompasses experimental and theoretical evaluation of the relative importance of solid decomposition, gas-phase reactions, and heterogeneous reactions in composite solid propellant ignition and combustion processes. The objective is to determine overall reaction paths and key kinetic factors, and to use these data to develop consistent ignition models. Ignition characteristics of conventional composite solid propellants and model polymer-oxidizer composite systems are being examined in a shock tube and in an arc-imaging furnace. Investigation of the effects on ignition time of formulation variables, inert and reactive gas environments, pressure, and flux level are currently being conducted. Thermal and thermal oxidative degradation behavior of polymers are being studied in a shock tube and flash pyrolysis apparatus. This report summarizes recent results of these investigations.

2.0 EXPERIMENTAL APPARATUS AND RESULTS

2.1 SHOCK TUBE

During the second year of this research program, the interaction of oxygen and various polymeric materials was investigated in the shock tube. A variety of fuels, exhibiting a spectrum of thermal and oxidative degradation characteristics, were selected for study. Thermoplastic materials utilized included polyethylene, polypropylene, and polystyrene, while PBAN, CTPB, and PIB represented typical elastomeric fuel components of conventional solid propellants.

The fuel samples were pressed or cast directly into a 3/8-in.-diameter stainless steel holder. All the tests were conducted with flush-mounted end-wall samples and tailored interface conditions identical to those used in the propellant ignition investigations.[1]*

2.2 ARC-IMAGING FURNACE

An arc-imaging furnace is a convenient tool for ignition research because the external heating rate can be controlled completely independently of other factors. Therefore, the observed effects of pressure, gaseous environment, propellant formulation variables, and heating rate can be assessed and directly related to the ignition process. However, the use of radiant energy as the ignition stimulus may introduce chemical and physical factors peculiar to this energy source, and identification and evaluation of these factors is being attempted in this program by systematic variation of propellant composition and test conditions. The experimental program is designed to obtain information on propellant ignition by the determination of ignition times for various formulations and by a photographic study of the overall radiative ignition sequence. Specific details of the UTC arc-imaging furnace are provided in reference 2.

Ignition time, τ_{ign}, has been obtained by using the go/no-go criterion. In this procedure, successive samples are exposed to energy pulses of known intensity and duration, and successful or unsuccessful ignition is

---

* Parenthetical superscript numbers denote references appearing on page 42.

noted. At low pressures, where ignition times are quite long, the exposure time was held constant and go/no-go limits of pressure were determined as a cross-check.

Test samples were discs of propellant 0.3-in. in diameter by 0.5 to 0.75-in. in thickness. A cork borer was used to cut specimens from a sheet of propellant prepared with a microtome knife. This procedure provided good reproducibility of sample surface. A nitrogen gas environment surrounded the samples in all tests.

A variety of propellant formulations were employed. All formulations utilized bimodel AP (70/30 coarse:fine), 0.25% iron oxide, and a total solids loading of 84%. PBAN, CTPB, PIB, and PU polymers were used as the binders. The influence of aluminum and carbon addition was also assessed. Ignition data for all propellants are summarized in tables I, II, III, and IV of appendix A. Ignition times exhibited scatter due to variations between specimens, and 20 individual tests were used as a minimum to establish a threshold. At some combinations of flux and pressure, it was necessary to use additional tests to maintain consistent reliability. The values reported for the flux assume unit absorptivity of the propellant surface. This is a reasonable assumption for propellants containing aluminum and carbon, but, of course, it is not valid for transparent formulations.

The second phase of the arc-imaging furnace investigation was concentrated on photographic studies to supply visual data regarding the overall radiative ignition process. High-speed photography as well as schlieren methods were employed. Two camera positions were selected for the high-speed photography. The first viewed test samples through a central opening in the reimaging mirror, permitting a direct frontal view of the propellant surface. The second position, from the side, allowed a 90° change of view which would show phenomena occurring at or near the propellant surface. For schlieren photography, the side position was used exclusively. Details of photographic techniques are presented in appendix B.

3.0 DISCUSSION

3.1 SHOCK TUBE STUDIES

A description of the response of a polymer surface to an ignition stimulus is an important factor in existing theories of composite solid propellant ignition.[1,3,4] For the specific case where oxygen is used as the external gaseous oxidizer, surface and gas-phase reaction models have been proposed to explain the observed influence of oxygen on the ignition time. Results of solid propellant and polymer ignition studies, using a shock tube as the experimental tool, have been employed to test both models.[1,4] However, these studies and data obtained by conventional decomposition techniques have not clearly demonstrated the validity of either approach. Rates of thermal decomposition of polymers are quite low at the initial surface temperatures produced in the shock tube, and a combustible gas-phase mixture may not be formed. On the other hand, the nature and rate of oxygen attack on polymer surfaces in the shock tube environment has not been clearly demonstrated and doubt exists as to whether the energy necessary to ignite a propellant can be generated by a surface reaction.

It was believed that clues to the relative importance of the thermal and thermal-oxidative processes under shock tube reaction conditions could be obtained by investigating the surface structure of polymers exposed to oxygen concentrations both above and below those required to ignite a propellant. A variety of polymer materials, displaying a range of thermal and oxidative stabilities, were exposed to various oxygen concentrations using the same shock tube experimental configuration and procedures employed for propellant ignition tests.[1] Following the tests, the polymer surfaces were examined with the aid of a stereo microscope.

Tables I and II summarize the surface structural characteristics noted in the microscopic examination. Ignition was detected by the light sensors only at oxygen concentrations exceeding $3 \times 10^{-3} g/cc$, in general agreement with the limiting concentration ($2 \times 10^{-3} g/cc$) observed in the propellant ignition studies.[1] While this experimental method provides only qualitative information, the results have provided insight into the probable importance of the thermal and surface-oxidative processes in the ignition of the different polymer systems in this particular experimental configuration.

4

TABLE I

SUMMARY OF THERMOPLASTIC FUEL IGNITION TESTS

Fuel	Test Gas	Test Pressure (P_5), psia	C_{ox}, g/cc	Surface Characteristics
Polyethylene	N_2	450	-	Evidence of melting and flow.
	Air	450	1.36×10^{-3}	Evidence of melting. A few brown-black spots on surface.
	O_2	450	6.5×10^{-3}	Ignition. Two distinct surface structures. *
	Air	630	1.9×10^{-3}	Melting and appearance of carbon in molten areas.
	O_2	630	9.1×10^{-3}	Ignition. Two distinct surface structures. *
	Air	925	2.8×10^{-3}	Melting and surface is about 85% to 90% covered with a "wet" brown-black material.
	O_2	925	13.3×10^{-3}	Ignition. Two distinct surface structures. *
Polypropylene	N_2	555	-	Evidence of melting and flow.
	10% O_2/90% N_2	555	0.8×10^{-3}	Evidence of melting. A few grey-black spots on surface.
	25% O_2/75% N_2	555	2×10^{-3}	Evidence of melting. Surface has "spotted" appearance. Irregular shaped grey areas partially cover sample surface.
	50% O_2/50% N_2	555	4×10^{-3}	Ignition. Two distinct surface structures. *
	70% O_2/30% N_2	555	5.6×10^{-3}	Ignition. Two distinct surface structures. *
Polystyrene	N_2	450	-	Slight melting.
	O_2	330	4.7×10^{-3}	Ignition. Two distinct surface structures. *
	O_2	380	5.4×10^{-3}	Ignition. Two distinct surface structures. *
	O_2	630	9.1×10^{-3}	Ignition. Two distinct surface structures. *

---

* In the tests where ignition occurred, the two distinct surface structures which were visible under microscopic examination had the following appearance:

    1. A dry, grey-black carboneous upper crust which covers the sample surface except where the crust has been blown away by gases evolving from the subsurface.

    2. A glossy, molten appearing, subsurface layer beneath the upper crust. In this layer, there are two color patterns. One is a yellow-brown area and the other a fine "grained" black carboneous area. The latter predominates in polystyrene.

5

TABLE II

SUMMARY OF ELASTOMERIC FUEL IGNITION TESTS

Fuel	Test Gas	Test Pressure (P_5), psia	C_{ox}, g/cc	Surface Characteristics
PBAN	N_2	560	-	No visible change.
	Air	765	2.3×10^{-3}	No visible change.
	O_2	390	5.6×10^{-3}	Ignition. Two distinct surface structures. *
	O_2	515	7.4×10^{-3}	Ignition. Two distinct surface structures. *
	O_2	725	10.0×10^{-3}	Ignition. Two distinct surface structures. *
CTPB	N_2	765	-	No visible change.
	Air	765	2.3×10^{-3}	No visible change.
	O_2	390	5.6×10^{-3}	Ignition. Two distinct surface structures. *
	O_2	515	7.4×10^{-3}	Ignition. Two distinct surface structures. *
	O_2	765	11×10^{-3}	Ignition. Two distinct surface structures. *
PIB	N_2	765	-	No visible change.
	Air	765	2.3×10^{-3}	No visible change.
	O_2	390	5.6×10^{-3}	Ignition. Two distinct surface structures. *
PIB	O_2	515	7.4×10^{-3}	Ignition. Two distinct surface structures. *
	O_2	680	9.7×10^{-3}	Ignition. Two distinct surface structures. *

---

* In the tests where ignition occurred, the two distinct surface structures which were visible under microscopic examination had the following appearance:

1. A grey-black carboneous upper crust covering a portion of the sample surface. At equivalent oxygen concentrations, the PIB displayed significantly less carboneous material in comparison to the PBAN and CTPB.

2. A glossy, molten appearing, subsurface layer beneath the upper crust. Subsurface layer is covered by a network of various size bubbles.

As shown in tables I and II, differences were noted in the surface structures of the thermoplastic and elastomeric systems at oxygen concentrations below those required to cause ignition. The thermoplastic polymers exhibited a molten surface. This suggests that one of the following sequences is the key kinetic reaction leading to ignition of the thermoplastics:

A. Vaporization of the liquid surface followed by a gas-phase reaction

B. Gas-liquid surface reaction.

McAlvey, et al,[5] have conducted experiments which help to distinguish between the possible reaction sequences. In these experiments, small beads of polystyrene enclosed in Pyrex tubing, initially charged with nitrogen at atmospheric pressure, were preheated to 220°C and abruptly exposed to oxygen at 220°C and 200 psi. The molten polystyrene failed to ignite, flash, or produce any sign of reaction. At equivalent oxygen concentrations and initial solid surface temperatures in the reflected shock wave, ignition occurs in a few milliseconds. The main difference is that the reflected shock gas temperature is of the order of 1,450°K compared to 220°C for the gas in the Pyrex tubing equipment. A combustible mixture apparently is not formed in the absence of the high gas temperature, and ignition does not occur. Although some gas-liquid reaction may take place, it is not sufficiently exothermic to lead to ignition. Therefore, it seems reasonable to assert that, in the shock tube environment, vaporization followed by a gas-phase reaction appears to be the principal reaction sequence for fuels that exhibit a molten surface.

However, the observations on the elastomeric polymers (table II) indicate that a molten surface prior to ignition is not a general characteristic of the polymer surface conditions in the shock tube environment. No evidence of melting or any changes in surface structure were noted for these materials at oxygen concentrations below the lower limit value. Thus, the possibility of oxygen attack on the surface cannot be ruled out. Furthermore, for an adsorption process following an equation of the form:

$$r_{ad} = \frac{aP}{(2\pi m k T_g)^{1/2}} \; f(\theta) \; e^{-E_{ad}/R T_s} \tag{1}$$

where

r_{ad} = number of molecules adsorbed per second per unit area

α = condensation coefficient

P = partial pressure of adsorbate in gas phase

m = molecular weight of adsorbate

T_g = gas temperature

$f(\theta)$ = chance that a molecule will strike an empty site

T_s = solid surface temperature

the rate of oxygen adsorption in the shock tube environment may exceed that at ambient conditions by a factor of 40 to 100 times.

Cheng, Ryan, and Baer[6, 7] investigated propellant ingredient decomposition for time intervals of interest in propellant ignition and their results indicate that gas-solid reactions may occur before ignition in some fuel systems. In their studies, thin films of polymers were mounted on thin discs of copper, the surface of the films was exposed to uniform thermal radiation, and the time-temperature relationships obtained from the copper discs were used to calculate significant reaction temperatures and magnitudes of the thermal reactions in or near the thin test films.

Tests on a typical PBAN polymer used in propellant formulations were conducted at pressures from 0.01 to 5 atm, and nitrogen and oxygen were used as environmental gases. The following conclusions were drawn:

A.   Significant surface regression of this polymer appears to start at about 390 °C.

B.   Exothermic oxygen-polymer reactions apparently occur before ignition.

C.   Ignition in oxygen appears to occur just after regression of the polymer begins.

Pearson and Sutton also investigated the ignition of composite propellant fuels by oxygen.[8] The oxidizer was directed either into a 2-1/4-in.-long, 1/2-in.-diameter Pyrex tube containing a sample of the fuel heated by a nichrome wire, or onto an unheated sample of fuel placed on a small watchglass at a distance of 1 in. from the tube outlet. The fuels used were polyisobutene, polyurethane, polystyrene, and polymethylmethacrylate. All experiments were conducted at atmospheric pressure. No ignitions were achieved with oxygen at temperatures in

the range of 200° to 300°C. Ignitions were achieved with oxygen only at temperatures well above 300°C, and in some cases, temperatures above 400°C were required. These temperatures are in agreement with those reported by Cheng, Ryan, and Baer. The requirement of a high temperature to achieve ignition indicates that gas-phase reactions are dominant at the oxygen concentrations used by these investigators.

However, neither of these experiments exactly duplicates the oxygen concentrations produced in the shock tube. The oxygen concentrations are lower by a factor of 2 to 3 than those in the shock tube, and the oxygen adsorption rate may be below that required to support a surface reaction. Thus, no definite conclusion can be drawn from these studies about the relative importance of a gas-solid reaction in the ignition of nonmelting fuels under the shock tube experimental conditions.

The possibility of a surface reaction, sufficiently exothermic to influence the ignition process in the shock tube environment, will be dependent upon the physical state of the fuel surface and the local molecular oxygen concentration. If a liquid or semifluid surface exists, a significant energy contribution by an oxygen-fuel surface interaction is doubtful. If a solid surface exists, energy contribution by a gas-solid reaction cannot be discounted on the basis of current knowledge. However, if an oxygen-solid fuel reaction does occur, it is doubtful that it could supply sufficient energy to result in ignition in the shock tube in the absence of energy transfer from subsequent gas-phase reactions. Furthermore, the shock tube generates a rather extreme oxygen concentration which is not representative of normal rocket motor igniter environments, and at atmospheric pressure, although some oxygen-solid fuel reactions might occur, they are certainly of little importance.

3.2 ARC-IMAGING FURNACE STUDIES

A majority of practical igniters do not produce oxidizing gases. In this situation, both the fuel and oxidizer molecules must originate from the propellant itself, and their subsequent chemical interaction provides the requisite energy to establish combustion. This phenomenon of heat release only from the propellant ingredient decomposition processes at a rate sufficient to achieve steady-state combustion is defined as the ignition response of the propellant.

Although it is an oversimplification, it is useful to consider the problem of the ignition of solid propellants as primarily one of production of volatiles. The process can be further defined by the consideration of two separate stages; (1) propellant heatup and (2) ignition of the volatiles following heatup. The overall ignition event can be divided into time

intervals representing these stages

$$\tau_{ign} = t_T + t_c \tag{2}$$

where

τ_{ign} = total time to ignition

t_T = time of propellant heating by external energy source alone

t_c = time of heat addition by various chemical reactions plus time of transition to steady-state combustion.

Since the chemical reactions associated with t_c are generally activated processes, the rate of volatiles generation rises rapidly with temperature and will flash through any threshold value within a small temperature rise. Therefore, ignition will usually occur when the solid reaches some fixed temperature and this temperature will be substantially independent of heating rate and other parameters over a limited range. This expectation has been substantiated by experimental data gathered in several programs on solid propellant ignition. [9]

However, if a complete understanding of the ignition mechanism is to be attained, the chemical time, t_c, must be defined in greater detail. The arc-imaging furnace studies are designed to explore the interrelationships among ignition characteristics and propellant compositional factors in order to determine chemical reaction sequences that may be important in determining t_c. This information will be used to guide the refinement of a model of the ignition process which was recently formulated. [1]

3.2.1 Photographic Investigations

High-speed photographic investigations were conducted to obtain qualitative data on propellant ingredient decomposition and the overall ignition process in the arc-imaging furnace. Tests were conducted on different polymer systems and a variety of composite AP propellant formulations using both normal high-speed photography and schlieren techniques.

In the standard ignition time measurements, when the sample is inserted in the holder, it is pushed snugly against a stainless-steel shield with a 0.25-in. circular aperature. The shield prevents heating of the specimens edges from the incident radiation. Photographic tests were

conducted both with and without this shield. The absence or presence of the shield had no apparent effect on the behavior noted in the following paragraphs.

Marked differences were observed in the behavior of the various propellants. The PIB-based propellant exhibited considerable surface bubbling activity and the surface had a definite molten appearance prior to ignition. The PU formulations exhibited some surface bubbling, but not nearly to the extent of the PIB systems. PBAN and CTPB-based propellants, on the other hand, displayed little, if any, surface bubbling prior to ignition.

All propellant systems exhibited binder pyrolysis or vaporization throughout the latter portion of the heating cycle. The vapor had the general characteristics of a smoke cloud, similar to those produced when a polymer has undergone a thermal cracking reaction. In many of the photographed ignition sequences, this smoke cloud was rapidly dispersed just prior to the appearance of a gas-phase flame. This dispersal was attributed to the vaporization of liquid drops in the smoke cloud by energy released in gas-phase preignition reactions. Sutton and Wellings[10] have reported similar findings in their investigation of solid propellant ignition by radiant energy. The photographs in figure 1 illustrate this sequence.

A gas-phase flame was the first observed indication of ignition in some tests, while in other instances surface "hot spots" were noted before the appearance of a gas-phase flame. When surface "hot spots" preceded the gas flame, particles ejected from the surface ignited the volatiles. This sequence is shown in figure 2 for an aluminized PIB propellant.

Figures 3 and 4 illustrate the ignition of a CTPB propellant as recorded by simultaneous visible and schlieren photography.

3.2.2 Ignition or Exposure Time Data

The ignition behavior of representative composite propellants was investigated as a function of incident radiant energy level and pressure. The pressure effect on ignition or exposure time is conveniently depicted by plots of log τ_{ign} versus log P, while the solution of the simple thermal ignition model suggests several representations for the flux dependence. A logarithmic plot in the form $(\tau_{ign})^{1/2}$ versus F tends to minimize experimental scatter in the ignition time. A plot of τ_{ign} versus F^2 on log coordinates provides a better picture of the experimental scatter in the measured ignition times even though it magnifies errors in the flux measurements. A third form, resulting from a plot of $(\tau_{ign} \times F)$ versus F presents

Figure 1. Ignition Sequence for PBAN Propellant
(Flux — 25 cal/cm²-sec)

Figure 2. Ignition Sequence for Aluminized PBB Propellant
(Flux — .25 cal/cm² - sec)

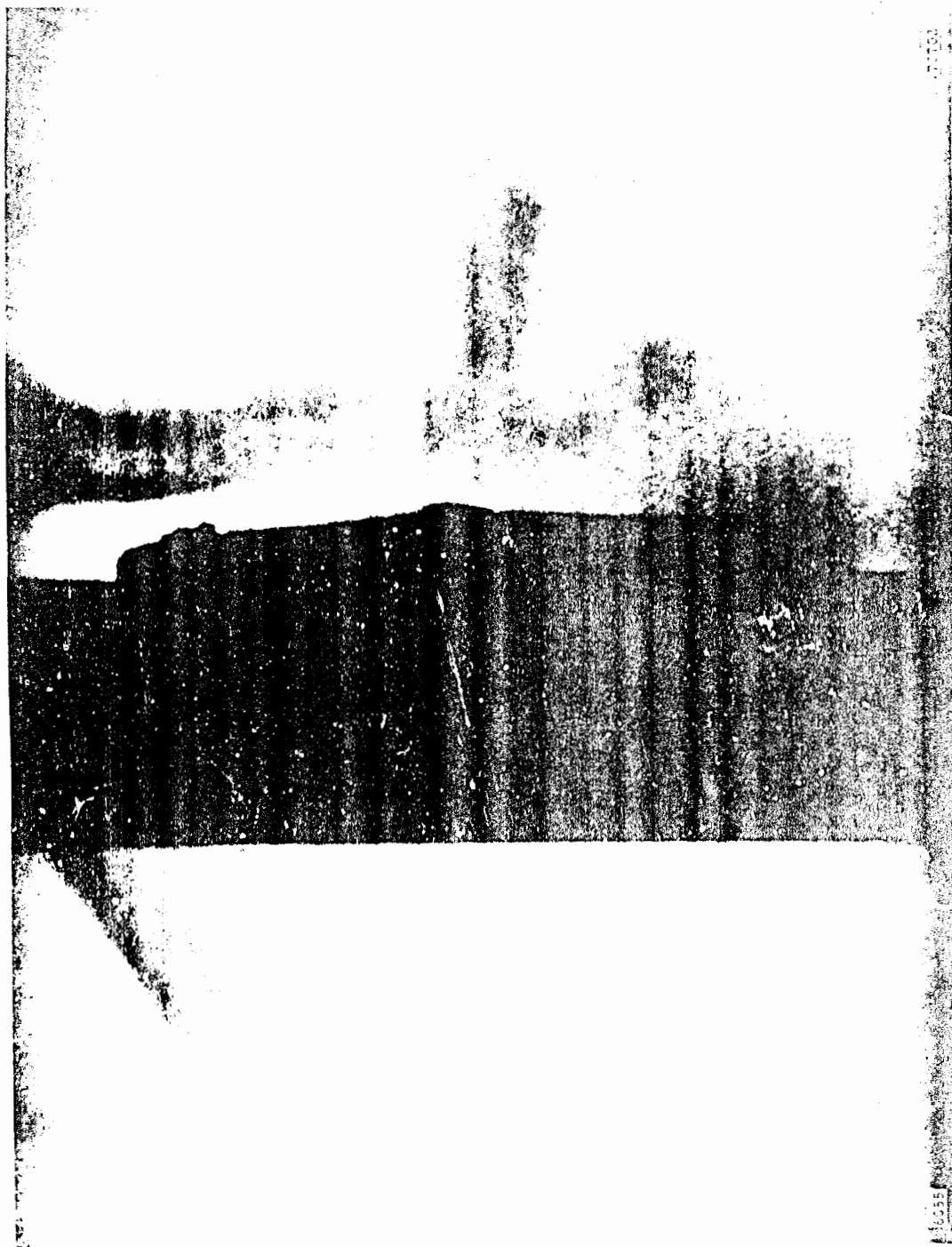Figure 3. Ignition of CTPB Propellant – Visible Photography

Figure 4. Ignition of CTPB Propellant – Schlieren Photography

a clear picture of the total energy requirements, although ignition times are not readily apparent. The second representation was selected for use in this report.

Figures 5, 6, 7, and 8 illustrate the pressure effect on ignition time for PBAN, CTPB, PU, and PIB propellants containing no aluminum or carbon, and figures 9, 10, 11, and 12 depict the flux dependence. Of course, these two forms of data presentation merely demonstrate the same behavior patterns from alternate viewpoints. The upper bound of the go/no-go limit was plotted. Since the data were not to be used to rigorously check a theoretical model or derive kinetic constants, but rather to guide the formulation of a mathematical model of ignition response, statistical techniques such as that developed by Evans[11] were not applied to the data. Reproducibility of the test results at identical flux and pressure points is good and we have confidence in individual data points.

The flux dependence plots indicate that in general the data are fit by a line of slope equal to -2.0 at flux levels below 20 to 25 cal/cm^2-sec and pressures above 0.5 to 0.75 atm. Outside these bounds, wide deviations from this limiting slope are observed. The limiting slope of -2.0 indicates that a constant surface temperature at ignition could be assumed in this flux-pressure range.

Figure 13 compares the effect of formulation factors on the ignition time of the PBAN propellant at a flux level of 58 cal/cm^2-sec. As is apparent, the ignition delay time decreases as the propellant is made more opaque by the addition of aluminum and carbon. Figure 14 shows the effect of 16% aluminum on the ignition characteristics of PU propellant at a flux level of 26 cal/cm^2-sec. As was the case with the PBAN system, the addition of aluminum decreases the ignition time at all pressures investigated.

Figure 15 depicts the effect of polymer variation on the ignition time for an incident flux level of 14 to 15 cal/cm^2-sec. Figure 16 shows a similar comparison for a flux level of 58 to 60 cal/cm^2-sec. The propellants contain 0.2% carbon and 0.25% iron oxide.

An examination of the ignition data indicates that the addition of aluminum and carbon and the variation of the fuel constituents have a pronounced influence on the ignition time. As shown in figures 13 and 14, aluminum and carbon decrease the ignition time, but do not alter the general shape of the τ_{ign} versus P plots. The principal effect of these additives can be attributed to changes in the propellant optical absorption characteristics.

16
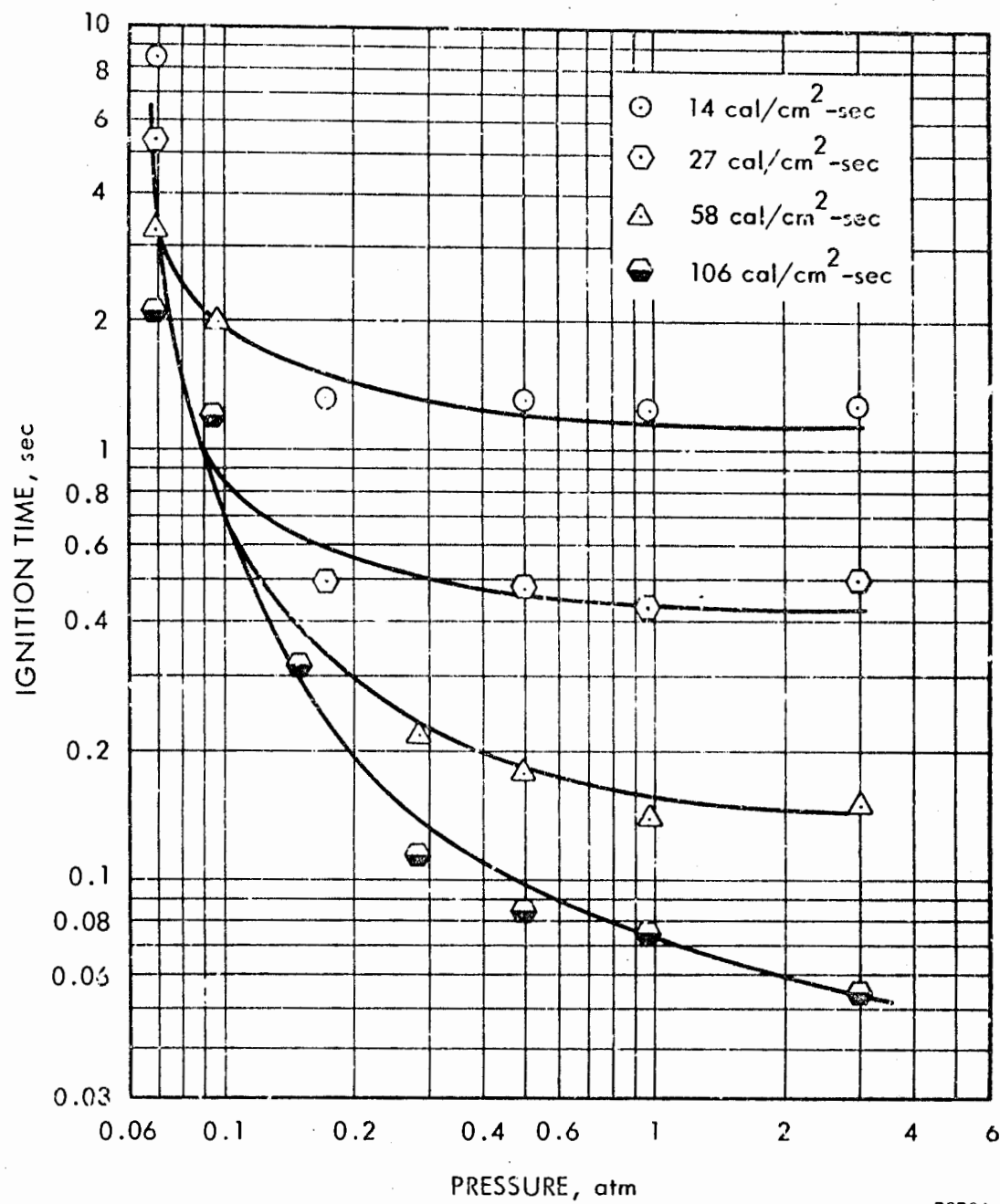
Figure 5.   Ignition Time as a Function of Pressure —
Nonaluminized PBAN Propellant

70703

17
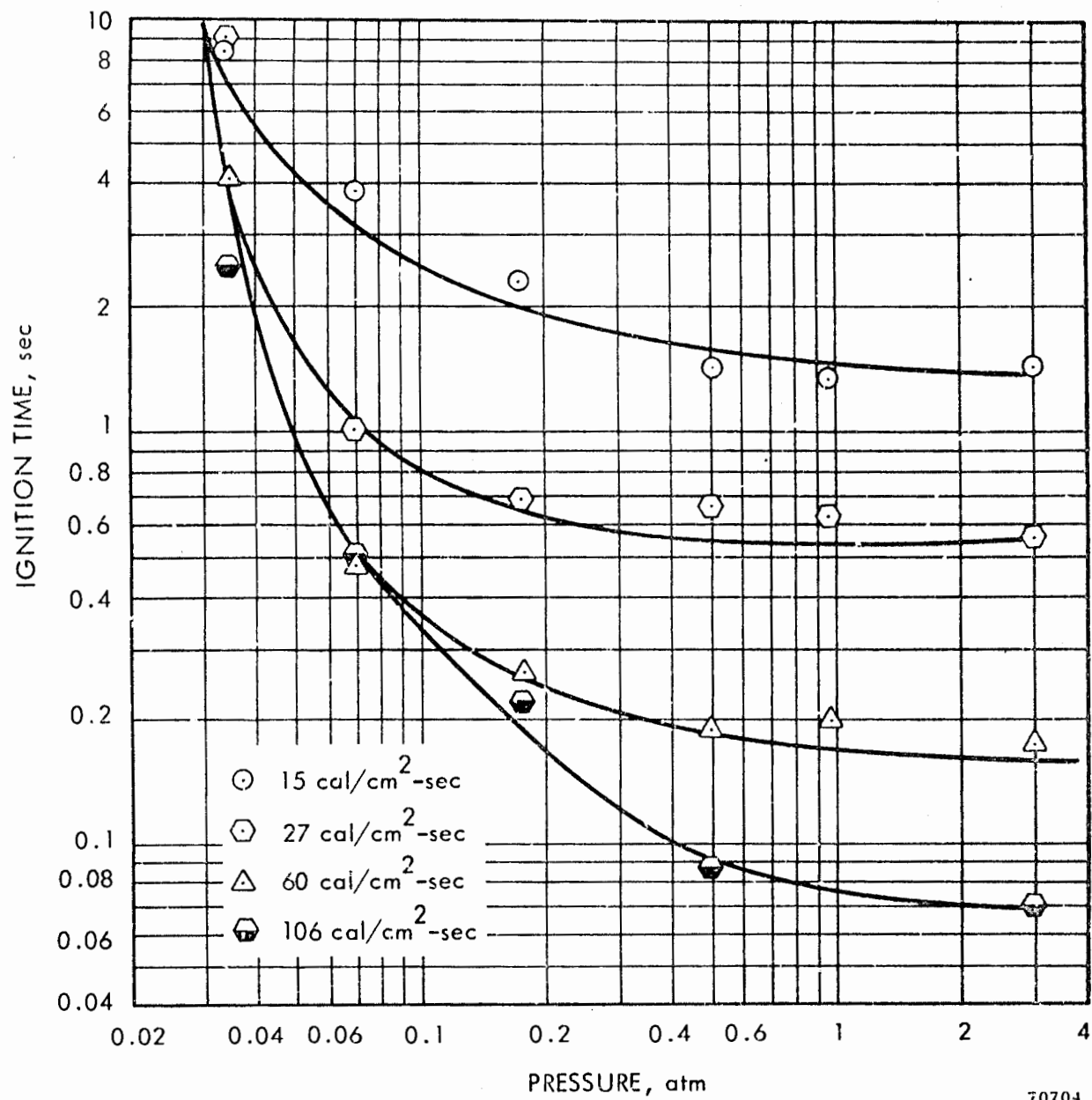
Figure 6. Ignition Time as a Function of Pressure —
Nonaluminized CTPB Propellant

70704
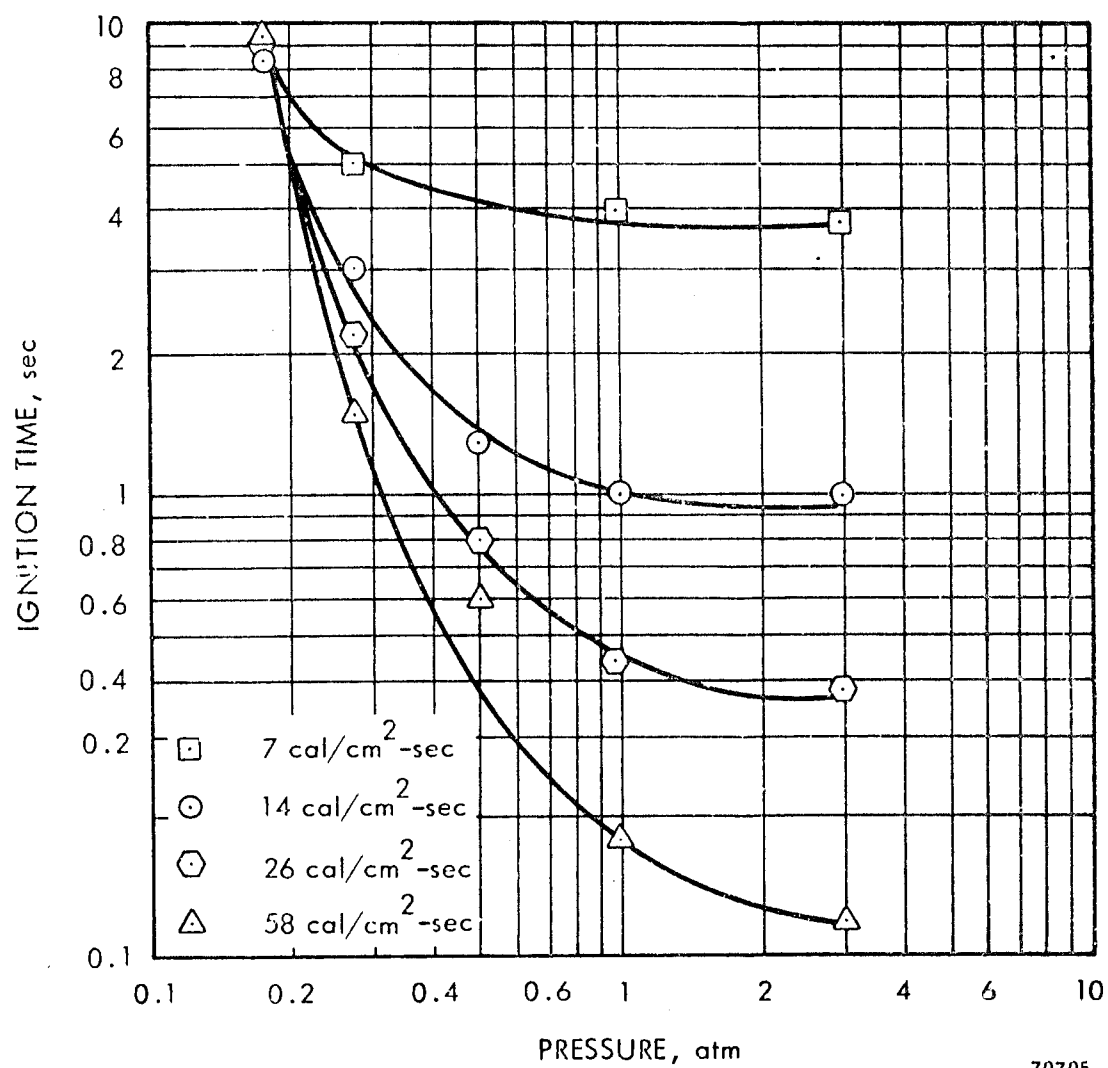
Figure 7. Ignition Time as a Function of Pressure —
Nonaluminized PU Propellant

70705

19
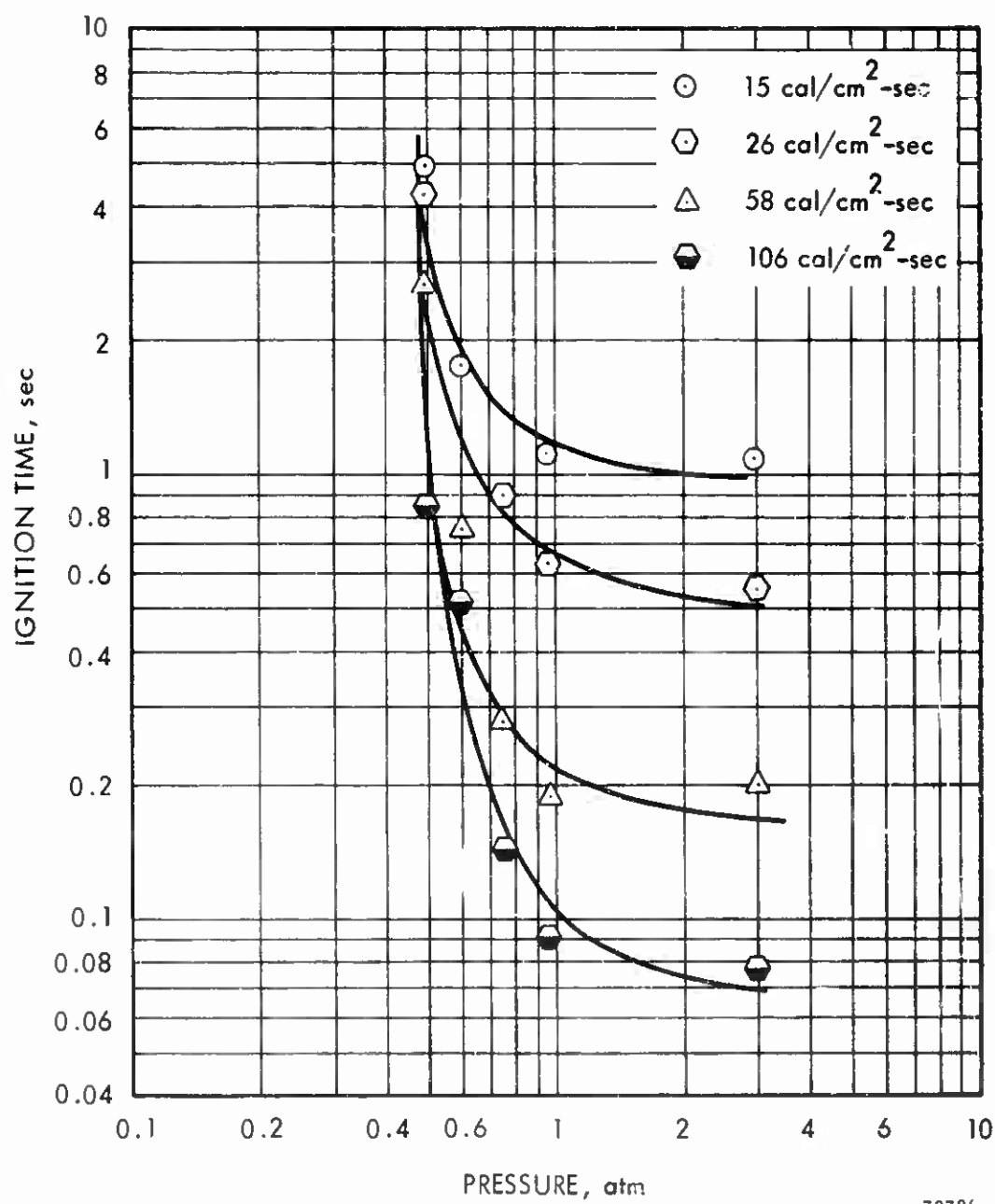
Figure 8. Ignition Time as a Function of Pressure —
Nonaluminized PIB Propellant

20
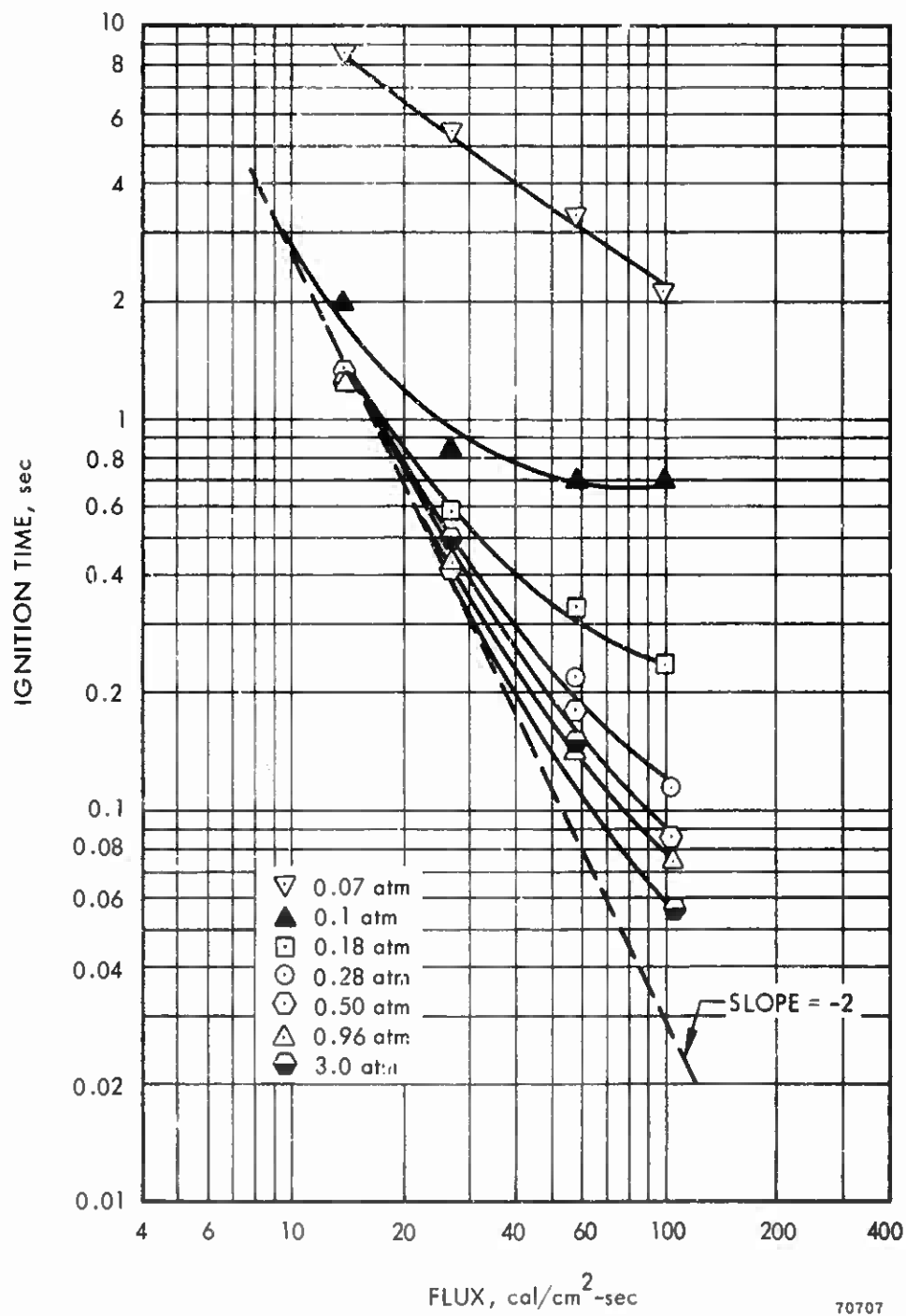
Figure 9. Ignition Time as a Function of Flux —
Nonaluminized PBAN Propellant

70707
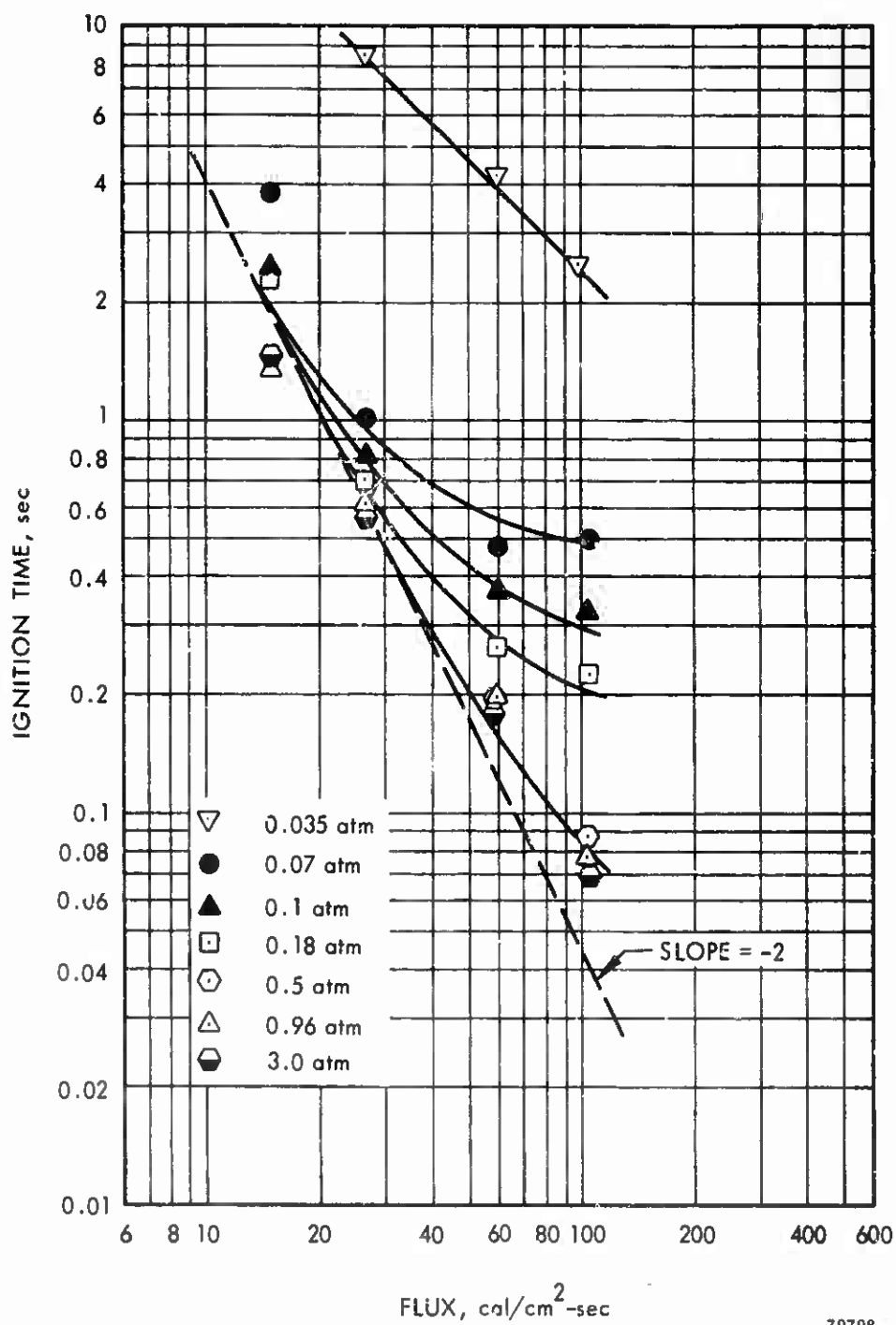
Figure 10.   Ignition Time as a Function of Flux —
Nonaluminized CTPB Propellant
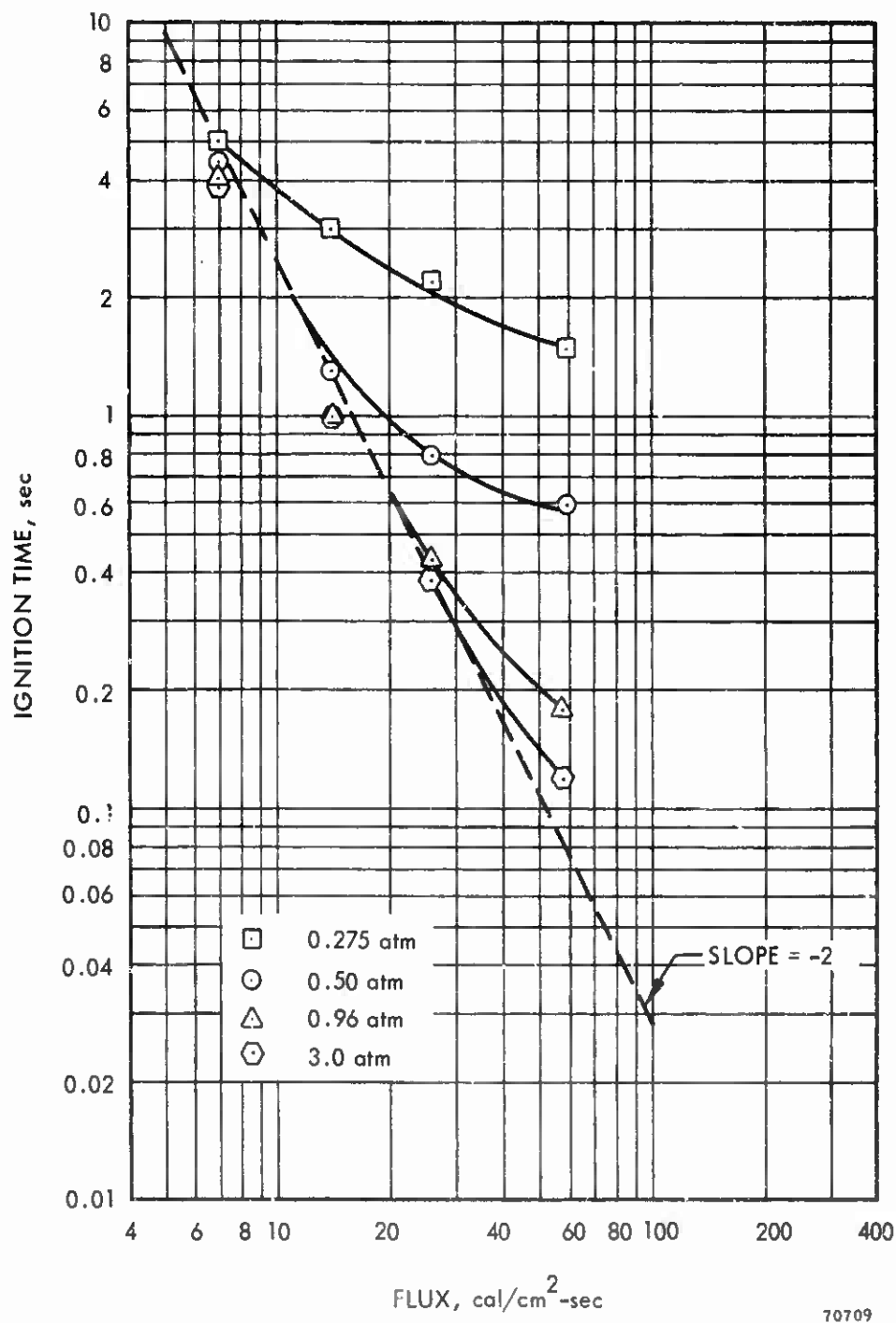
Figure 11. Ignition Time as a Function of Flux —
Nonaluminized PU Propellant

70709
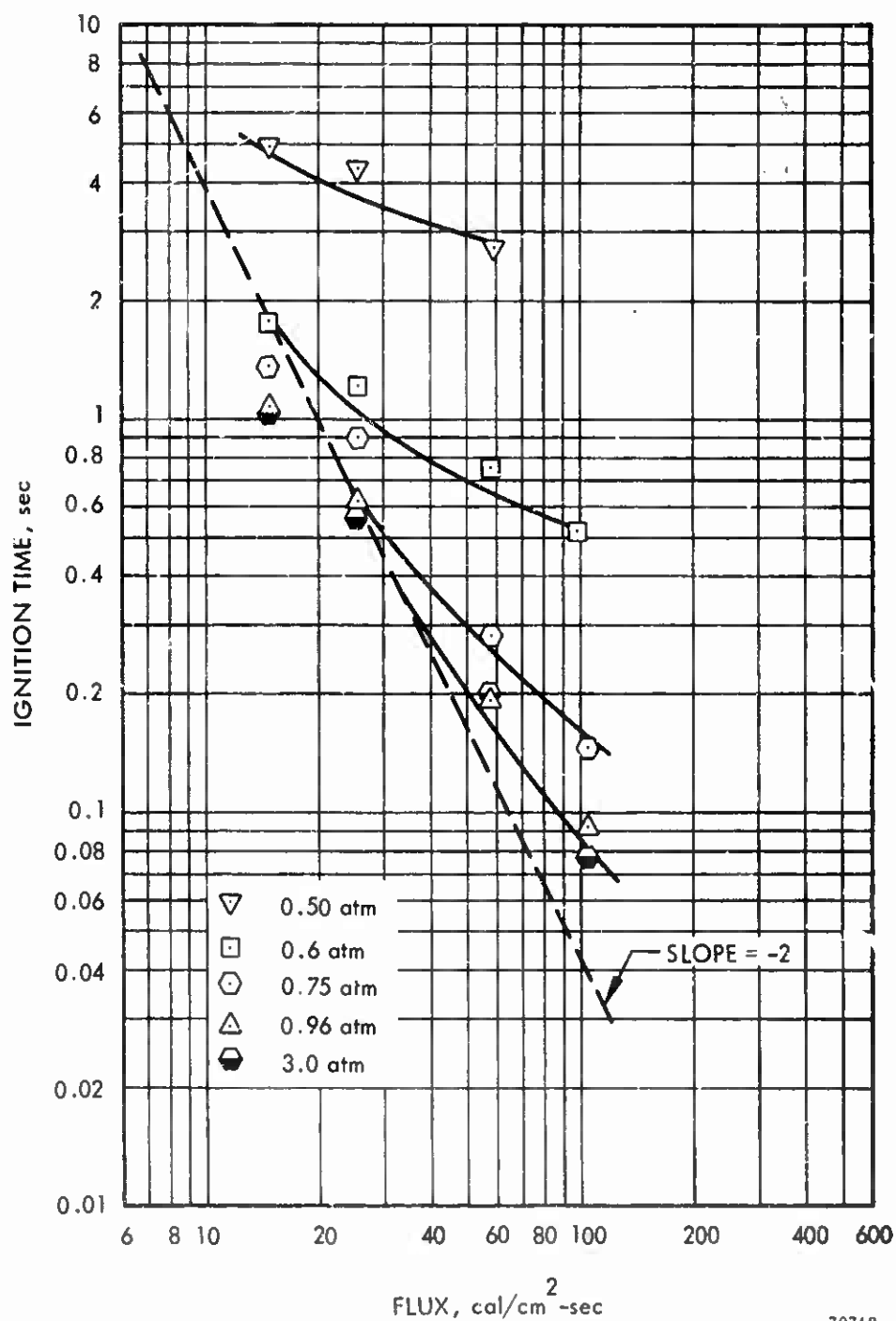
Figure 12. Ignition Time as a Function of Flux —
Nonaluminized PIB Propellant

24
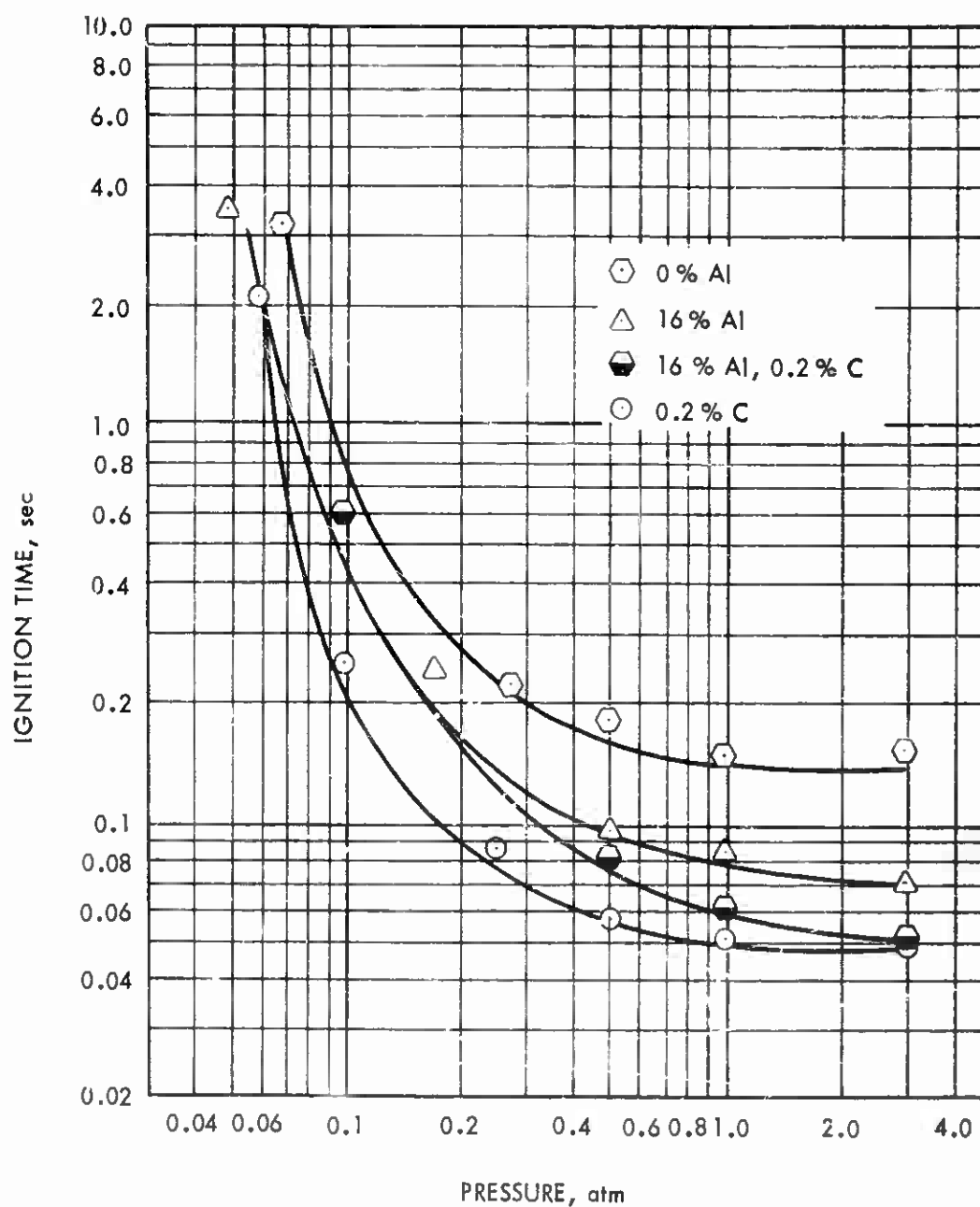
Figure 13. Effect of Formulation Factors on Ignition Time
of PBAN Propellant (Flux — 58 cal/cm²-sec)
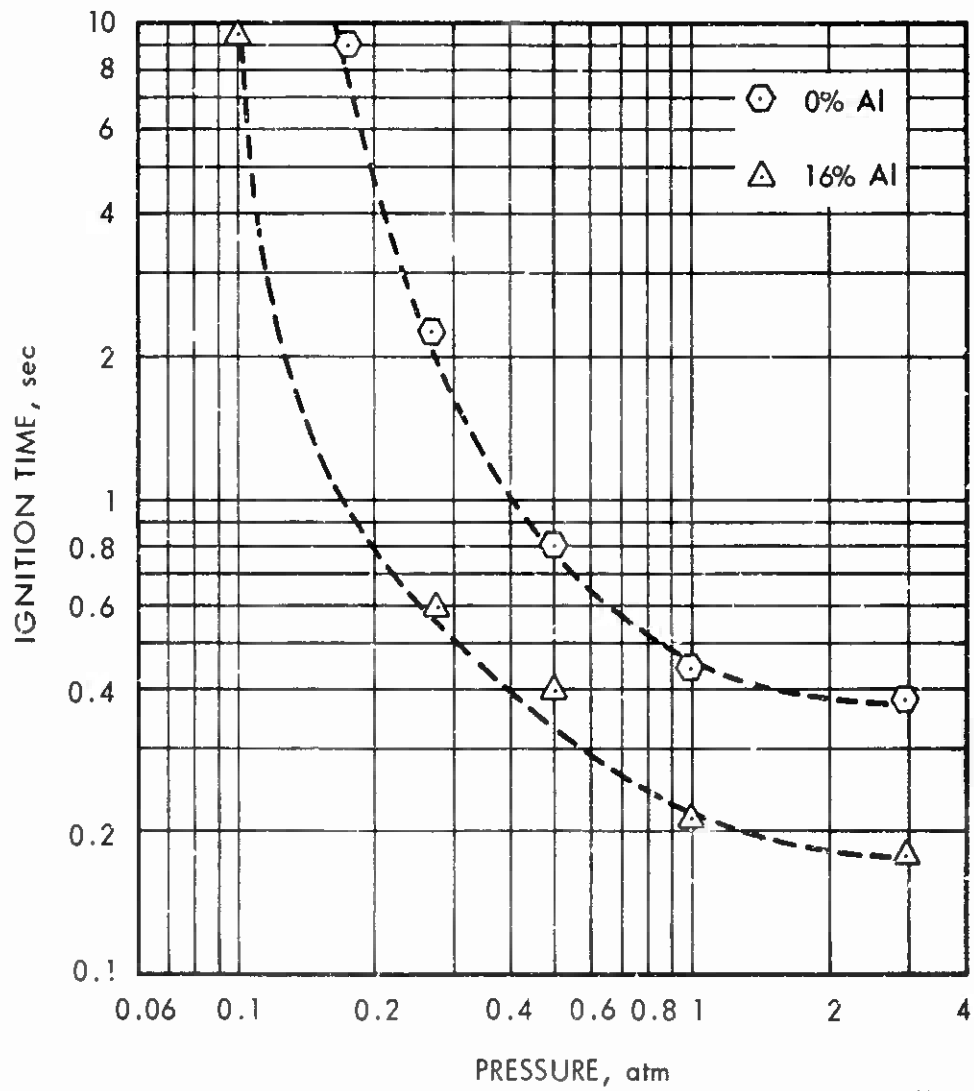
Figure 14. Effect of Formulation Factors on Ignition Time
of PU Propellant (Flux — 26 cal/cm²-sec)

70711
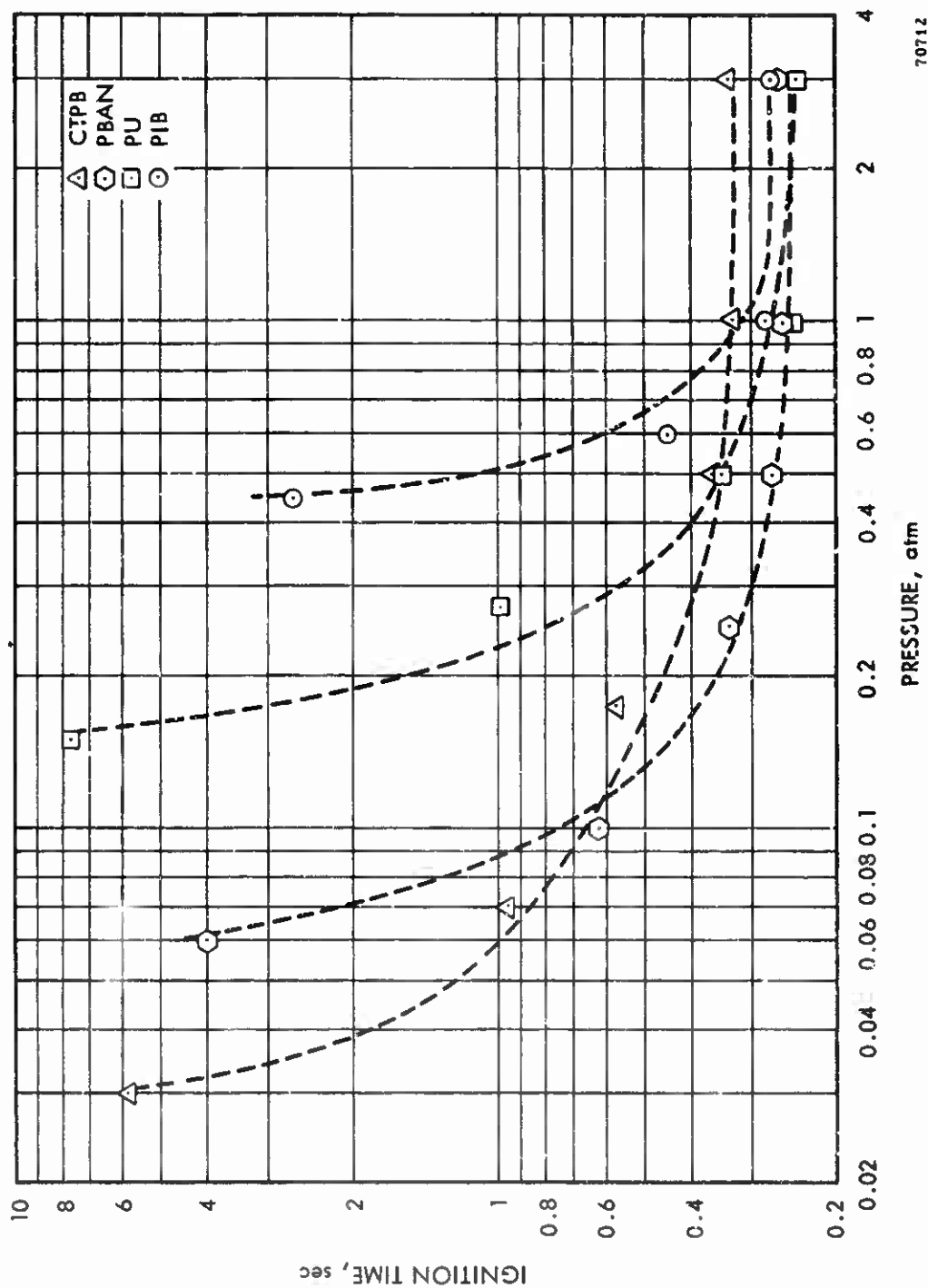
Figure 15. Effect of Polymer on Ignition Time (All Propellants — 0.2% C, Flux 14 to 15 cai/cm²-sec)

70712

27
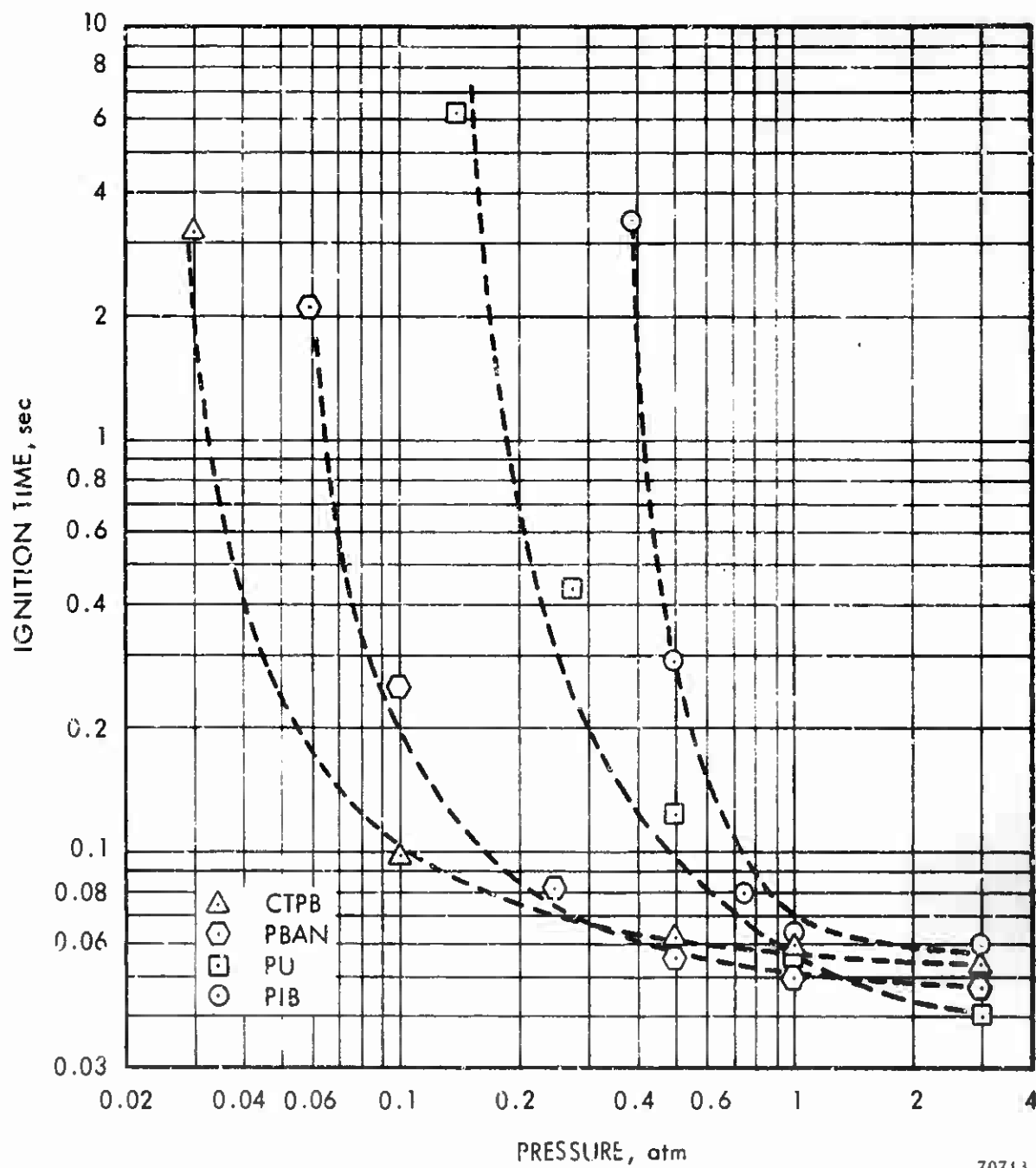
Figure 16. Effect of Polymer on Ignition Time
(All Propellants — 0. 2% C, Flux 58 to 60 cal/cm^2-sec)

70713

The influence of fuel variation seems to be related to the initial pressure. Two distinct regions of pressure-fuel interaction are discernible from figures 15 and 16:

A. Ignition times show a strong dependence on the nature of the fuel element at pressures below approximately 0.75 atm, and the minimum pressure at which ignition occurs is sensitive to fuel variations.

B. Ignition times exhibit little dependence on the fuel component at pressures above 1 atm.

The most notable influence of polymer variation occurs with regard to the minimum ignition pressure. Changes in minimum ignition pressure can be correlated with the thermal stability (as determined by bulk decomposition techniques) of the polymer. The CTPB polymer has the highest thermal stability (i.e., highest decomposition temperature) of the four fuels, and propellants formulated with this polymer exhibit the lowest minimum ignition pressure. PBAN is more stable than PU, and PBAN propellants display a lower minimum ignition pressure than PU propellants. PU, in turn, has a higher decomposition temperature than the PIB, and a lower minimum ignition pressure results for the PU propellants.

Since the minimum ignition pressure is determined by an energy balance at the propellant surface, the volatilization or pyrolysis reactions of the polymer would be expected to play an important part in establishing the limiting pressure. The extent to which polymer pyrolysis diverts energy from the surface heating process will be the key factor, and a propellant whose binder is more difficult to decompose will exhibit a lower limiting pressure than a propellant whose binder is more readily decomposed.

At pressures above the minimum ignition pressure, and below 0.75 atm, ignition time is also dependent upon the chemical nature of the fuel element and, presumably, its thermal and oxidative degradation characteristics. Since the thermal decomposition of the fuel is endothermic, and the heat of decomposition of AP is endothermic below approximately 300 mm Hg, [12] a heat balance at the propellant surface is again the primary factor in the ignition process. If the external energy plus that generated by gas-phase and interfacial chemical reactions does not exceed the surface endotherms, ignition isn't achieved because the surface temperature cannot attain a sufficiently high level.

Above approximately 0.75 atm, ignition times exhibit little dependence on the fuel structure at all the flux levels employed. Autoignition

temperatures, calculated from the general heat conduction equation in the absence of chemical reaction (shown in table III) indicate that, at low flux levels, the majority of the measured ignition time can be attributed to propellant heating by the external energy source. However, at the higher flux levels, autoignition temperatures determined in this manner are not realistic, and attention must be directed to the chemistry and reaction kinetic aspects (i.e., to t_c).

The following sequences are potentially the key kinetic reactions influencing t_c in catalyzed propellants:

A. Chemical reaction between perchloric acid or its decomposition products and the solid polymer

B. Exothermic decomposition of perchloric acid and ammonia on the surface of the iron oxide catalyst

C. Gas-phase reaction between perchloric acid or its decomposition products and gaseous ammonia or other fuel molecules.

The oxidative degradation characteristics of the polymers in the various formulations are sufficiently different so that a more noticeable difference in ignition time might be anticipated if a gas-solid reaction were the principal kinetic factor. However, perchloric acid is a very reactive oxidizer and it may not show any selectivity among the polymers used in this study.

Pearson and Sutton[13] have reported on an investigation of the ignition characteristics of perchloric acid vapor with: (1) solid fuels with low vapor pressures, and (2) gaseous fuels expected to be formed during the ignition phase of an ammonium perchlorate-polyisobutene propellant. With the solid fuels, heated perchloric acid vapor was directed into a Pyrex tube containing a sample of the fuel placed on a watch glass. Carbon, nylon, sugar, charcoal, and polyurethane ignited readily at times and temperatures similar to those obtained with composite propellants. Ammonia, methane, ethylene, and isobutene were used as gaseous fuels, and streams of perchloric acid vapor and selected fuel gases, heated to various initial temperatures, were mixed or allowed to impinge upon a ceramic tile, a hotplate, or various potential catalysts and the ignition delay was determined. No ignitions were observed in the absence of a surface or a catalyst (copper chromate or ferric oxide) and the order of ignitability was found to be ammonia>isobutene>ethylene> methane. When copper chromate was present, ammonia at 200° to 300°C ignited very rapidly with no noticeable delay. Ferric oxide was as

TABLE III

AUTOIGNITION TEMPERATURES

Propellant	Flux cal/cm^2-sec	T_{Ai}, °C
CTPB (0.2% carbon)	15	421
PBAN (0.2% carbon)	14	342
PU (0.2% carbon)	14	330
PIB (0.2% carbon)	15	376

effective a catalyst for the ammonia-perchloric acid ignition as copper chromate, but titanium dioxide, silica, and alumina did not produce a detectable reduction in the ignition delay over that noted for the ceramic or hotplate surfaces. It was found that the perchloric acid-ammonia-catalyst mixtures ignited faster than perchloric acid-solid fuel mixtures. Rosser, et al, have also suggested the importance of the catalysis of perchloric acid-ammonia ignition by copper chromate.[14]

These results indicate that various types of heterogeneous reactions can be important in composite propellant ignition if sufficient concentrations and temperatures are available at the appropriate reaction sites. Unfortunately, very little is known about the concentrations and temperatures at the solid interfaces during propellant ignition, and no definitive conclusion can be reached regarding what heterogeneous reactions may occur.

The gaseous fuel pyrolysis products of polymers used in the propellants are quite similar and their reactivity with perchloric acid should be nearly equivalent. Thus, the observed independence on the nature of the fuel specie might also be explained on the basis of gas-phase reactions being the most important chemical reaction. Furthermore, since it is expected that heterogeneous reactions in the absence of a subsequent gas-phase flame would not actually result in a successful ignition (i.e., establishment of steady-state burning), it is not realistic to discount contributions due to gas-phase reactions.

In the absence of more detailed kinetic data, it is difficult to assess the relative importance of the various reaction mechanisms. Interfacial reactions will depend upon the local concentration of reactive gases and the existence of a solid (polymer or catalyst), or possibly a liquid fuel, at the interface. The local reactive gas concentration will be determined in turn by the oxidizer decomposition rate and diffusion into the surrounding gas. The physical state of the fuel at a binder/oxidizer interface will be determined by its thermal decomposition characteristics. The initiation of a flame in the volatiles immediately adjacent to the surface, in the absence of some piloting mechanism, depends upon the attainment of a sufficient temperature of the volatiles mixture, plus the establishment of at least a flammability limit. These conditions are determined by the rates and energetics of the oxidizer and binder decomposition process, the pressure, gas-phase chain branching reaction rates, and heat losses.

Objectively, it must be considered that no single controlling chemical mechanism can be proposed and it is likely that interfacial, catalytic, and gas-phase reactions each contribute energy to the ignition process. For a specific case, the relative importance of any single reaction process will

depend upon interrelated factors such as local concentrations, local temperatures, interface chemical and physical structure, external heating rate, and external pressure. A reasonable comprehensive analytical model must be used in conjunction with experimental ignition and kinetic data to establish the roles of various unit processes over the complete spectrum of pressure and heat flux. Preliminary work in this direction is discussed in section 4.0.

3.3 SUMMARY OF ARC-IMAGING FURNACE RESULTS

General characteristics noted in the ignition time and photographic data are:

A. The logarithmic plots of τ_{ign} versus P are curves bounded by an asymptote of infinite slope at the minimum ignition pressure, and an asymptote of zero slope in the pressure independent (high pressure) regime.

B. Binder type appears to be the predominant formulation variable influencing the minimum ignition pressure in the AP-based formulations.

C. The minimum ignition pressure does not appear to be a function of incident radiant flux, at least in the ranges' examined to date.

D. Variation of the minimum ignition pressure with binder type follows the same order as the thermal stability of the polymer (i.e., increasing the polymer thermal stability lowers the minimum ignition pressure).

E. Ignition times show a strong dependence on the nature of the fuel element at pressures below approximately 0.75 atm, but exhibit little dependence at pressures above 1 atm.

F. Neither the thermal nor oxidative degradation character-istics of the polymers appear to influence strongly the ignition time at pressures of the order of 1 atm.

G. Ignition times decrease as the propellant is made more opaque by the addition of aluminum or carbon.

H. Gasification of the polymer element begins early in the heating cycle.

I.   A molten layer may exist on some propellant surfaces
     prior to ignition.

3.4   FLASH PYROLYSIS AND GAS FLOW APPARATUS

Flash pyrolysis and gas flow equipment were designed and constructed during this period.   This experimental equipment will be used to study propellant ingredient decomposition processes in time intervals of interest for propellant ignition.

The flash tube apparatus will be used to heat properly prepared solid materials very intensely and rapidly.   A flash discharge system.has, as shown in figure 17, four essential items: a dc power supply, a capacitor bank, a starter system, and a flash discharge tube.   The electronic circuitry used in this flash tube system is of conventional type with one important difference.   This system has been designed with appropriate components such that the power dissipated through the flash lamp due to the capacitor bank discharge is essentially a square power pulse and hence the sample being irradiated is exposed to a constant heat flux over the duration of the test.

The circuit features inductor/capacitor (L/C) units shown on the schematic (figure 17) as C_i for the capacitors and L_i for the inductors. The capacitors (120μ farad) are a laser discharge type, and may be charged to 5 Kv.   The inductors were specially fabricated and are rated at 7.8 millihenries.   The system presently has the capability of six L/C units.   Two typical units are shown in figure 17.   The duration of the energy pulse is determined by the number of L/C units in the circuit with a maximum test time of 20 msec obtainable by using all six L/C units. The flash lamp starter unit is the trigger source for the energy discharge through the flash lamp which initially ionizes the gas within the lamp, allowing the capacitors to discharge their energy.   The capacitors are charged through a current-limiting resistor by a power supply continuously variable from zero to 5 Kv.   As a safety feature, a capaction discharge resistor is wired in parallel with each capacitor through a switch.

The gas flow equipment increases the number of variables that can be explored in the area of polymer and propellant susceptibility and response to reactive gaseous environments.   The system permits an examination of the response of the propellant or polymer surface to reactive gases delivered under various flow conditions.   The sample can be exposed to either (1) convective flow of gaseous reactants past the surface or (2) stagnation flow conditions during which the stream of reactant gases is impacted directly on the surface of the sample.
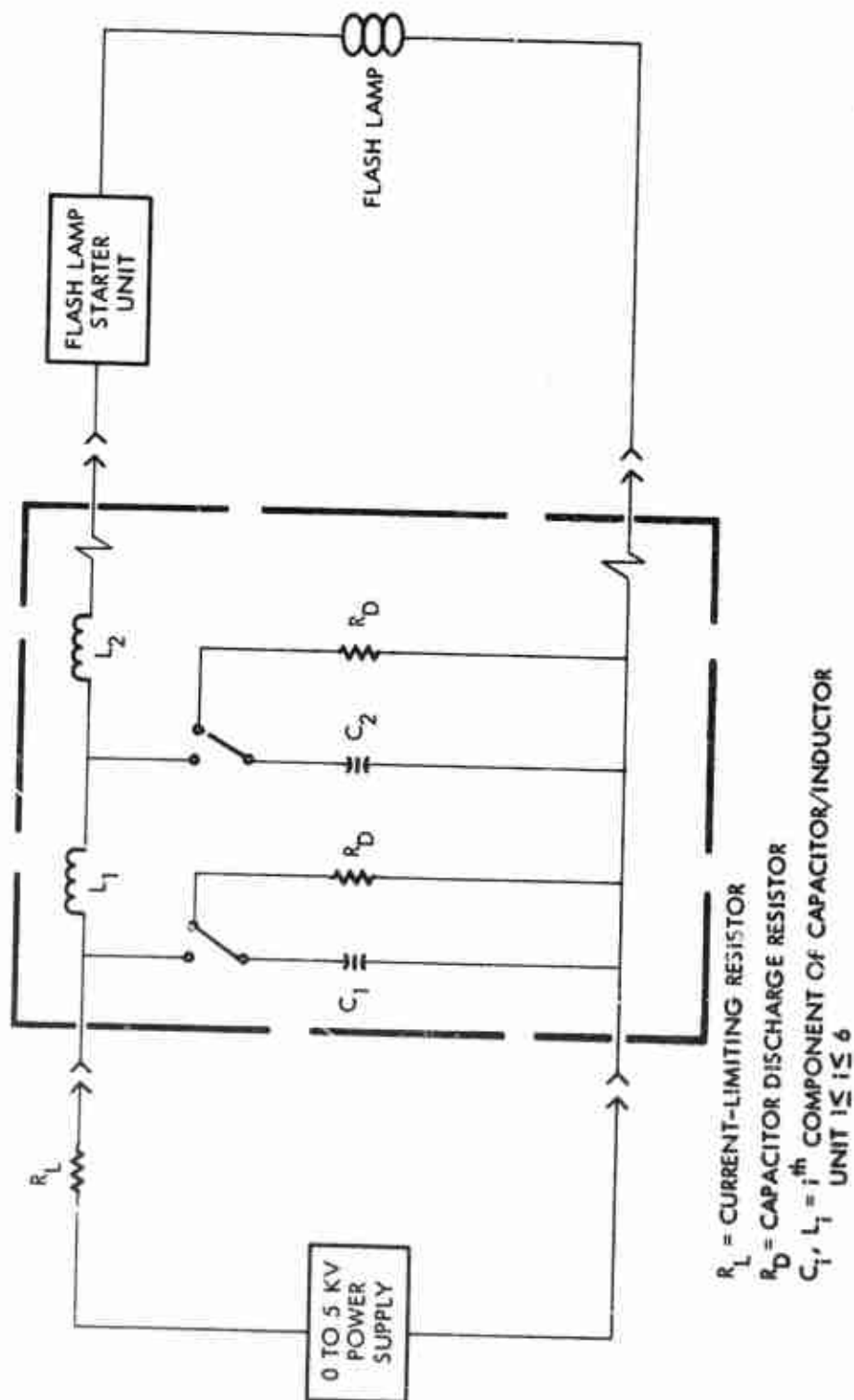
Figure 17. Flash Tube Electronic Circuit

R_L = CURRENT–LIMITING RESISTOR

R_D = CAPACITOR DISCHARGE RESISTOR

C_i, L_i = i^{th} COMPONENT OF CAPACITOR/INDUCTOR
UNIT $1 \leq i \leq 6$

70714

35

4.0 THEORETICAL IGNITION MODEL

This section outlines preliminary work on the formulation of an analytical model for composite solid propellant ignition in a neutral environment. Existing ignition theories do not provide a suitable framework for the interpretation of ignition data over the entire range of parameters of interest.

Figure 18 illustrates the general features of the model being developed and table IV summarizes the nomenclature. The coupled system of partial differential equations describing the model are given below. The derivation of these equations is well known and will not be repeated here.

A. Conduction of Heat in the Condensed Phase

$$\frac{\partial T_2}{\partial t} = \alpha_2 \frac{\partial^2 T_2}{\partial x^2} + I_o (1-r) \exp^-(x\beta) + v_2 \frac{\partial T_2}{\partial x} \tag{3}$$

where the regression velocity is given by

$$v_2 = \dot{m}/\rho_2 = (A_2/\rho_2) \exp(-E_2/RT_s) \tag{4}$$

B. Conduction of Heat in the Gas Phase

$$\frac{\partial T_1}{\partial t} + v \frac{\partial T_1}{\partial x} = \alpha_1 \frac{\partial^2 T_1}{\partial x^2} + (q/\rho_1 C_{P_1}) C_F C_{ox} A_1$$

$$\exp(-E_1/RT) \tag{5}$$

C. Surface Thermal Boundary Conditions

$$-k_2 \frac{\partial T_2}{\partial x} + \dot{m} C_{P_2} T_s = -k_1 \frac{\partial T_1}{\partial x} + \dot{m} C_{P_1} T_s + \Delta H_v \dot{m} \tag{6}$$

$$-I_o (1-r) - C_{ox} A_3 \Delta H_3 \exp(-E_3/RT_s) - A_4 \Delta H_4 \exp(-E_4/RT_s)$$
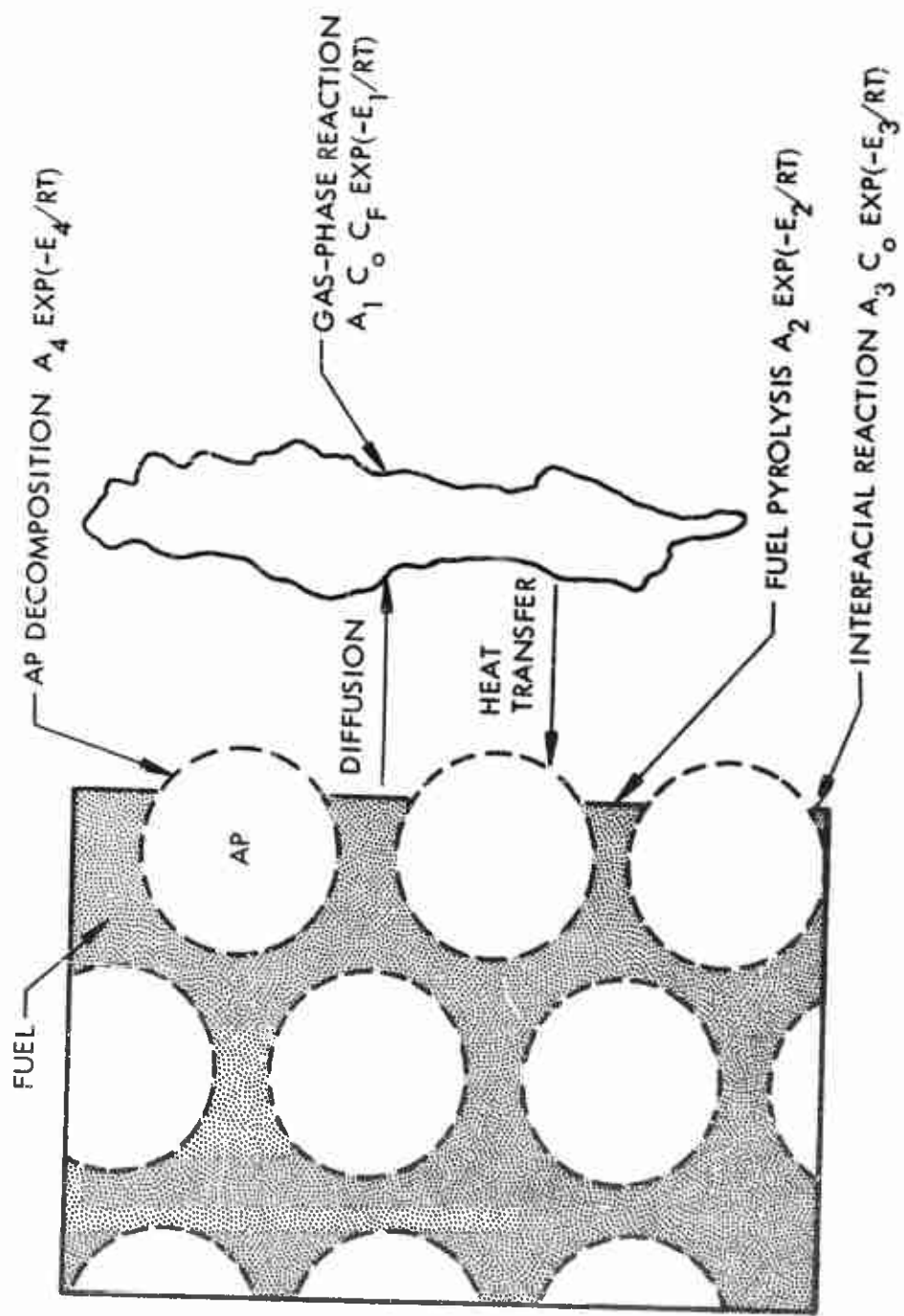
Figure 18. Ignition Model

D. Oxidizer Concentration Equations

$$\frac{\partial C_{ox}}{\partial t} = D \frac{\partial^2 C_{ox}}{\partial x^2} - C_F C_{ox} A_1 \exp(-E_1/RT_1) - v_1 \frac{\partial C_{ox}}{\partial x} \tag{7}$$

E. Oxidizer Boundary Condition at Interface of Gaseous and Condensed Phase

$$D \frac{\partial C_{ox}}{\partial x} = v_1 C_{ox} + A_3 C_{ox} \exp(-E_3/RT_s) - A_4 \exp$$

$$(-E_4/RT_s) \tag{8}$$

F. Fuel Concentration Equations

$$\frac{\partial C_F}{\partial t} = D \frac{\partial^2 C_F}{\partial x^2} - C_F C_{ox} A_1 \exp(-E_1/RT_1) - v_1 \frac{\partial C_F}{\partial x} \tag{9}$$

G. Fuel Boundary Condition at Interface of Gaseous and Condensed Phase

$$D \frac{\partial C_F}{\partial x} = v_1 C_F - A_2 \exp(-E_2/RT_s) \tag{10}$$

In order to systematically explore the above equations, we normalize these equations with respect to the solid phase reaction. Our method of analysis is unique insofar as solving coupled transient diffusion equations is concerned. First, a system of ordinary differential equations is generated from the relevant partial differential equations by discretization in terms of the space variable, and then the sequence of values of the dependent variable at the mesh points are regarded as new dependent variables. This leads to a system of ordinary differential equations (in derivatives with respect to time). This means of solution of boundary value problems has been extensively exploited in analogue computer work for solution of such problems as transient heat conduction, lateral vibration of beams, etc. In analogue work, the limitation is usually the capacity of the analogue computer. The relatively recent development of digital computer subroutines ("package solvers") for solution of large order systems of differential equations has brought "analogue discretization" methods into focus as a competitive means for solving certain types of partial differential equations.

The specific advantages of this approach to solution of boundary problems may be listed as follows:

A. The programming time is cut to a minimum since most of the difficult programming has been done in the ordinary differential equations subroutine itself. Also, the computer running time for the differential equations approach seems to offer an advantage compared to problems involving differencing in both the space and time steps.

B. Numerical convergence problems (i.e., convergence problems arising in numerical solution of the partial differential equations) are then related to problems of convergence of solutions of systems of ordinary differential equations. Most subroutines for solution of ordinary differential equations have some means of assurance of numerical convergence of the solution.

C. Conversion of a boundary value problem into a system of ordinary differential equations provides a means of handling nonlinear difficulties. This point is particularly important since many of our equations involve the exponential Arrhenius term as well as reactant product terms.

D. The capacity of the differential equation "package solvers" is large enough to allow use of a fairly large number of mesh points in the discretization.

The computer program is currently being "debugged" and parametric studies will begin following completion of this activity.

TABLE IV

IGNITION MODEL NOMENCLATURE

A_1, A_2, A_3, A_4	frequency factor (gas-phase, fuel pyrolysis, interface, and oxidizer decomposition reactions)
C_F, C_{ox}	concentration of fuel and oxidizer (gas phase)
C_{P_1}, C_{P_2}	specific heats
D	gas phase diffusivity (Lewis number = unity)
E_1, E_2, E_3, E_4	activation energies (gas-phase, fuel pyrolysis, interface, and oxidizer decomposition reactions)
I_o	incident radiant flux
k	thermal conductivity
$\dot{m}$	$A_2 \exp(-E_2/RT$ (fuel regression rate)
q	gas-phase heat of reaction
R	universal gas constant
r	reflectivity
$T_1(x, t)$, $T_2(x, t)$	temperatures (gas, condensed phase)
T_s	surface temperature
v_1	gas velocity
v_2	surface regression rate (velocity)
x	distance
α_2	condensed phase thermal diffusivity

TABLE IV

IGNITION MODEL NOMENCLATURE (Continued)

β	absorption coefficient
ΔH_3	heat of reaction
ρ	density
subscript 1	refers to gas phase
subscript 2	refers to condensed phase

REFERENCES

1. Shannon, L. J., "Composite Solid Propellant Ignition Mechanisms," AFOSR Scientific Report, AFOSR 66-2103, November 1966.

2. Beyer, R. B., et al, "Ignition of Solid-Propellant Motors Under Vacuum," United Technology Center Report, UTC-2079 FR, April 1965.

3. Anderson, R., et al, "Ignition Theory of Solid Propellants," Presented at AIAA Solid Propellant Rocket Conference, Palo Alto, Calif., 29 through 31 January 1964 (AIAA Preprint 64-156).

4. McAlevy, R. F., and M. Summerfield, "The Ignition Mechanism of Composite Solid Propellants," Aeronautical Engineering Report No. 557, Princeton University, 1 June 1961.

5. McAlevy, R. F., et al, Astronautica Acta 2: 144-145, 1965.

6. Cheng, J. T., A. D. Baer, and N. W. Ryan, "Thermal Effects of Propellant Component Reactions," Presented at 3rd ICRPG Combustion Conference, Cocoa Beach, Florida, 17 through 21 October 1966.

7. Ryan, N. W., et al, "Ignition and Combustion of Solid Propellants," AFOSR Report 40-64, University of Utah, 30 September 1964.

8. Pearson, G. S., and D. Sutton, AIAA Journal 4: 954-956, 1966.

9. Price, E. W., et al, "Theory of Ignition of Solid Propellants," Presented at AIAA 3rd Aerospace Sciences Meeting, New York, New York, 24 through 26 January 1966.

10. Sutton, D., and P. C. Willings, "Ignition of Solid Propellants by Radiant Energy," R.P.E. Report 66/4, Westcott, England, April 1966.

11. Evans, M. W., et al, "Error Analysis of Data from Arc Image Furnace Ignition Experiments," Presented at AIAA 2nd Propulsion Joint Specialist Conference, Colorado Springs, Colorado, 13 through 17 June 1966 (AIAA Preprint 66-669).

REFERENCES (Continued)

12. Wenograd, J., and R. H. W. Waesche, "Research Investigation of the Decomposition of Composite Solid Propellants," Quarterly Status Letter No. 1, July-October 1966.

13. Pearson, G. S., and D. Sutton, AIAA Journal 5: 344-346, 1967.

14. Rosser, W. A., et al, "Ignition of Simulated Propellants Based on Ammonium Perchlorate," Stanford Research Institute Report PU-3573, July 1965.

APPENDIX A

ARC-IMAGING FURNACE DATA

TABLE A-I

ARC-IMAGING FURNACE TESTS -
PBAN FORMULATIONS

Propellant	Pressure atm	Flux cal/cm^2-sec	Exposure Time sec
UTX-5123-Al (16% Al)	0.045	7	9.8 to 9.5
	0.045	14	5.5 to 5.4
	0.045	58	3.4 to 3.0
	0.07	7	4.05 to 3.9
	0.07	26	2.9 to 2.7
	0.07	58	3.3 to 3.0
	0.07	100	1.5 to 1.45
	0.1	14	1.6 to 1.4
	0.12	100	0.65 to 0.57
	0.175	7	3.0 to 2.8
	0.175	14	0.88 to 0.75
	0.175	26	0.4 to 0.32
	0.175	58	0.24 to 0.22
	0.275	26	0.3 to 0.27
	0.275	100	0.135 to 0.13
	0.5	7	2.8 to 2.6
	0.5	14	0.62 to 0.59
	0.5	26	0.23 to 0.22
	0.5	58	0.095 to 0.088
	0.5	100	0.060 to 0.054
	1.0	7	2.1 to 1.9
	1.0	14	0.62 to 0.60
	1.0	26	0.18 to 0.17
	1.0	58	0.083 to 0.080
	1.0	100	0.047 to 0.042
	1.2	58	0.075 to 0.069
	3.0	7	2.0 to 1.85
	3.0	14	0.6 to 0.55
	3.0	26	0.18 to 0.175
	3.0	58	0.070 to 0.065
	3.0	100	0.045 to 0.040

TABLE A-1

ARC-IMAGING FURNACE TESTS -
PBAN FORMULATIONS (Continued)

Propellant	Pressure atm	Flux cal/cm^2-sec	Exposure Time sec
UTX-5123	0.07	14	8.5 to 8.45
(0% Al)		27	5.4 to 5.3
		58	3.26 to 3.17
		106	2.1 to 2.06
	0.095	58	2.09 to 2.05
		106	1.2 to 1.1
	0.15	106	0.32 to 0.30
	0.175	14	1.3 to 1.25
		27	0.49 to 0.45
	0.275	58	0.22 to 0.213
		106	0.115 to 0.105
	0.5	14	1.29 to 1.24
		27	0.48 to 0.47
		58	0.179 to 0.165
		106	0.086 to 0.081
	1.0	14	1.25 to 1.20
		27	0.44 to 0.43
		58	0.14 to 0.135
		106	0.076 to 0.071
	3.0	14	1.25 to 1.20
		27	0.5 to 0.48
		58	0.15 to 0.147
		106	0.055 to 0.050
UTX-5123-C	0.06	14	4.0 to 3.9
(0.2% carbon)		57	2.1 to 2.0
	0.1	14	0.62 to 0.605
		57	0.25 to 0.24
UTX-5123-C	0.25	14	0.325 to 0.310
		57	0.083 to 0.075
	0.5	14	0.27 to 0.262
		57	0.056 to 0.051
	1.0	14	0.255 to 0.240
		57	0.050 to 0.046
	3.0	14	0.265 to 0.26
		57	0.047 to 0.0400

TABLE A-II

ARC-IMAGING FURNACE TESTS - CTPB PROPELLANT

Propellant	Pressure atm	Flux cal/cm^2 sec	Exposure Time sec
UTX-6519	0.035	15	8.5 to 8.4
		27	9.05 to 8.8
		60	4.15 to 4.0
		106	2.7 to 2.45
	0.07	15	3.8 to 3.76
		27	1.00 to 0.97
		60	0.49 to 0.45
		106	0.50 to 0.46
	0.175	15	2.3 to 2.27
		27	0.69 to 0.68
		60	0.264 to 0.26
		106	0.224 to 0.218
	0.5	15	1.42 to 1.405
		27	0.65 to 0.63
		60	0.190 to 0.186
		106	0.089 to 0.086
	1.0	15	1.335 to 1.315
		27	0.625 to 0.614
		60	0.199 to 0.196
	3.0	15	1.445 to 1.43
		27	0.56 to 0.54
		60	0.178 to 0.173
		106	0.07 to 0.065
UTX-6519-C (0.2% carbon)	0.03	14	5.9
		58	3.3
	0.07	14	0.95 to 0.93
	0.1	58	0.098 to 0.09
UTX-6519-C (0.2% carbon)	0.175	14	0.57 to 0.55
	0.5	14	0.36 to 0.35
		58	0.063 to 0.057
	1.0	14	0.325 to 0.32
		58	0.06 to 0.055
	3.0	14	0.335 to 0.32
		58	0.054 to 0.05

TABLE A-III

ARC-IMAGING FURNACE TESTS -
PIB PROPELLANT

Propellant	Pressure atm	Flux cal/cm^2-sec	Exposure Time sec
UTX-6094	0.5	15	4.91 to 4.83
		26	4.185 to 4.15
		58	2.68 to 2.62
		106	0.855 to 0.83
	0.6	15	1.76 to 1.70
		58	0.75 to 0.73
		106	0.507 to 0.49
	0.75	26	0.90 to 0.85
		58	0.283 to 0.277
		106	0.145 to 0.139
	1.0	15	1.105 to 1.045
		26	0.625 to 0.621
		58	0.185 to 0.177
		106	0.091 to 0.086
	3.0	15	1.08 to 1.05
		26	0.569 to 0.563
		58	0.20 to 0.185
		106	0.077 to 0.069
UTX-6094-C (0.2% carbon)	0.4	58	3.4 to 3.25
	0.45	15	2.65
	0.5	58	0.29 to 0.282
	0.6	15	0.42 to 0.405
	0.75	58	0.08 to 0.075
	1.0	15	0.28 to 0.274
		58	0.063 to 0.060
	3.0	15	0.27 to 0.265
		58	0.060 to 0.058

TABLE A-IV

ARC-IMAGING FURNACE TESTS -
PU PROPELLANT

Propellant	Pressure atm	Flux cal/cm^2-sec	Exposure Time sec	
UTX-7499	0.175	14	8.5	to 8.35
		26	9.0	to 8.8
		58	9.1	to 8.85
	0.275	7	5.0	to 4.78
		14	3.0	to 2.87
		26	2.2	to 2.05
		58	1.5	to 1.4
	0.5	14	1.3	to 1.15
		26	0.8	to 0.77
		58	0.6	to 0.57
	1.0	7	4.0	to 3.85
		14	1.0	to 0.975
		26	0.44	to 0.415
		58	0.18	to 0.165
	3.0	7	3.8	to 3.67
		14	1.0	to 0.9
		26	0.38	to 0.37
		58	0.12	to 0.10
UTX-7499-C	0.15	15	7.6	
		58	6.2	
	0.275	15	0.98	to 0.97
		58	0.44	to 0.425
	0.5	15	0.34	to 0.32
		58	0.125	to 0.11
	1.0	15	0.245	to 0.233
		58	0.057	to 0.05
	3.0	15	0.24	to 0.23
		58	0.04	to 0.036

TABLE A-IV

ARC-IMAGING FURNACE TESTS - PU PROPELLANT (Continued)

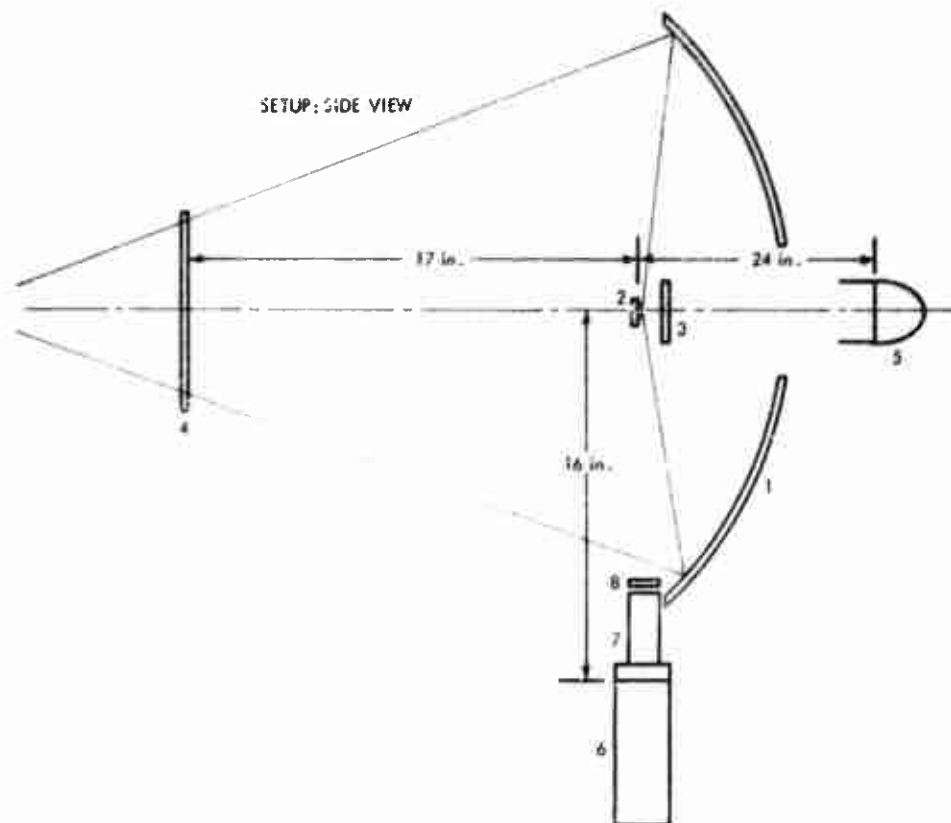| Propellant	Pressure atm	Flux cal/cm^2-sec	Exposure Time sec
UTX-7499-Al	0.1	26	9.5
		58	7.0
	0.175	58	0.53 to 0.50
	0.275	26	0.6 to 0.57
		58	0.19 to 0.18
	0.5	26	0.40 to 0.392
		58	0.15 to 0.143
	1.0	26	0.215 to 0.21
		58	0.095 to 0.09
	3.0	26	0.18 to 0.17
		58	0.063 to 0.059

APPENDIX B

PHOTOGRAPHIC TECHNIQUES

Investigation of the ignition process by photographic techniques was undertaken to supply visual qualitative data of propellant ignition in addition to the standard ignition time measurements. The primary objective of the photographic study was the detection and measurement of phenomena occurring on or near the surface of solid propellants prior to, during, and after ignition.

Visible and schlieren photography were used to record the ignition sequence. Two camera positions were used for the visible photography. The first viewed the test sample through a central opening in the re-imaging mirror. This position permits a direct frontal view of the propellant surface. The second position, from the side, allows a 90° change of view that would show phenomena occurring at or near the propellant surface. A Photo-Sonic camera was selected on the basis of the required frame rate, timing capability, and available optics.

During the arc exposure, certain ignition phenomena occurring on or near the propellant surface could not be recorded when camera exposure was set fo   he high intensity of the arc. The main problem was the visible light emitted by the arc. A Corning IR filter (7-56) which emits from 0.75μ to 4.50μ was placed in the low-intensity area of the arc-image path to remove the visible light. This method proved so effective that supplementary light had to be added to observe the test specimen before ignition, and it was necessary to add an event light to record shutter opening and closing. The camera exposure varies according to the type of propellant being tested.

A time base was recorded onto the film by the use of a pulse generator providing 100 cps pulse to a light mounted within the camera. This gives a constant time base regardless of any camera speed fluctuation. In addition, an event light records the opening of the arc-light shutter on the opposite side of the film. For most propellants, a frame rate of 500 frames per second was established as adequate. This allows a sufficient time expansion of the rapidly occurring events for qualitative analysis.

Schematics of the camera setup for the visible photography are presented in figures B-1 and B-2. Camera arrangement for the simultaneous visible and schlieren photography is presented in figure B-3.

SETUP: SIDE VIEW

CAMERA: 16 mm PHOTOSONIC

SHUTTER: No. 5 (72^c)

FILM: KODAK EFB (ASA 250) FORCED PROCESS

EXPOSURE: 1/2,500 sec at f/4.5 to f/16

NOTES: Exposure determined by test. In general: binder materials-f/4.5; nonaluminized
propellants-f/6.3; aluminized propellants-f/11 to f/16.

1	FURNACE REIMAGING MIRROR
2	PROPELLANT SAMPLE HOLDER
3	3/8-in. PLATE GLASS TO PROTECT MIRROR FROM COMBUSTION PRODUCTS
4	6-in.- SQUARE CORNING IR FILTER (7-56). FILTER REMOVES VISIBLE LIGHT FROM THE ARC SOURCE. FILTER IS COOLED BY NITROGEN JETS.
5	COLORTRAN PAR 64 OI NARROW SPOT. (10,600 lumens) 1,000 w
6	16 mm PHOTOSONIC CAMERA
7	6-in. FOCAL LENGTH TELEPHOTO LENS
8	+4 DIOPTER SUPPLEMENTARY LENS

T0716

Figure B-1. Photographic Setup for Side Shot
of Propellant Sample

SETUP: TOP VIEW

10 in.

2 3 4 5 6
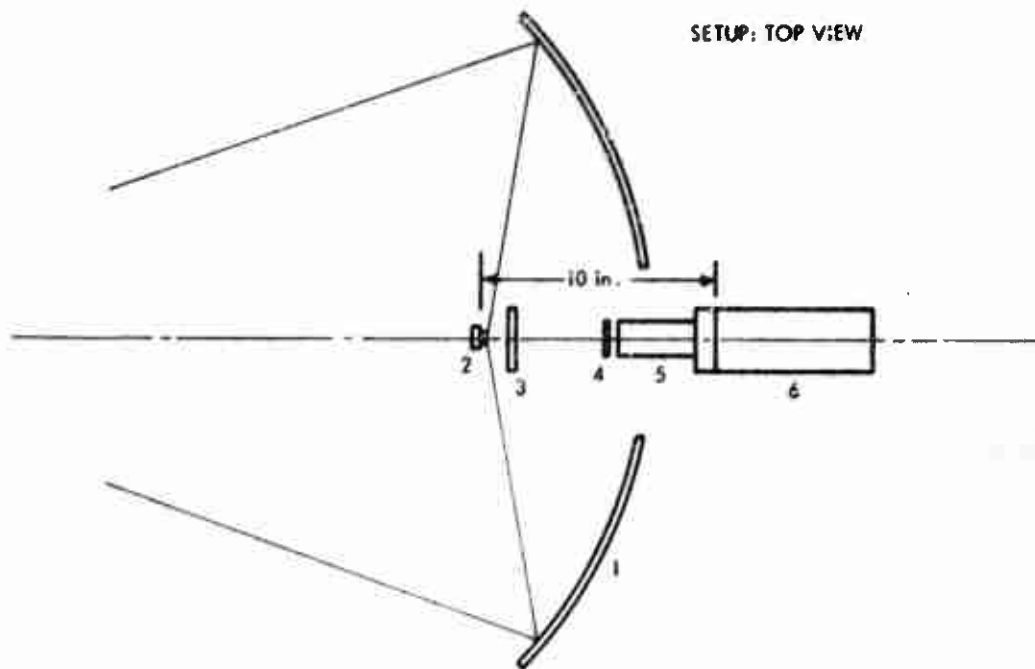
CAMERIA: 16 mm PHOTOSONIC

SHUTTER: No. 40 (9°)

FILM: KODAK EF (ASA 160)

EXPOSURE: 1/20,000 sec at f/22*

NOTES: *Exposure will vary as flux level of furnace arc source is changed.
This exposure was used at a flux of 5.

1   FURNACE REIMAGING MIRROR
2   PROPELLANT SAMPLE HOLDER
3   3/8-in. PLATE GLASS TO PROTECT MIRROR FROM COMBUSTION PRODUCTS
4   +10 DIOPTER SUPPLEMENTARY LENS
5   6-in. FOCAL LENGTH TELEPHOTO LENS
6   16 mm PHOTOSONIC CAMERA

70717

Figure B-2.   Photographic Setup for Front Shot
of Propellant Sample

SETUP: TOP VIEW

27 in.   15 in.   16 in.

7 in.

17 in.

DETAIL: SIDE VIEW

9 in.
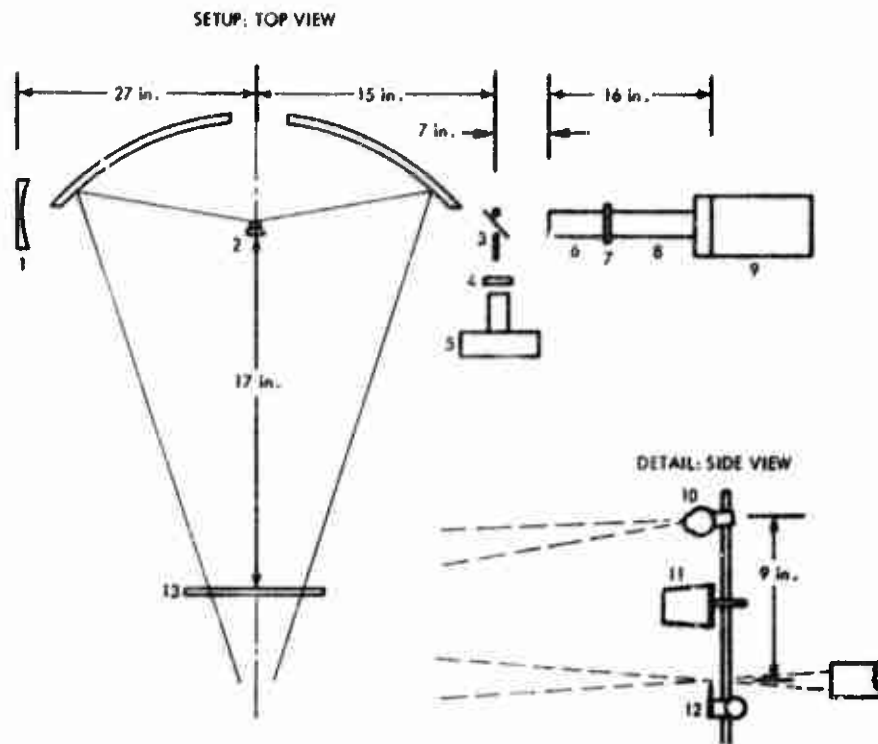
CAMERA: 16 mm PHOTOSONIC

SHUTTER: No. 5 (72°)

FILM: KODAK EFB (ASA 125)

EXPOSURE: 1/2,500 sec w/o 30
NEUTRAL DENSITY FILTER, 500 PPS

HYCAM 16 mm CAMERA

2:1

KODAK EFB (ASA 125)

1/1,000 sec at f/5.6, 500PPS

NOTES:

1   21-in. FOCAL LENGTH SCHLIEREN MIRROR

2   PROPELLANT SAMPLE HOLDER

3   POINT SOURCE, MIRROR, KNIFE EDGE (SEE DETAIL)

4   +2 DIOPTER SUPLEMENTARY LENS

5   HYCAM CAMERA WITH 2-in. FOCAL LENGTH LENS

6   12-in. FOCAL LENGTH TELEPHOTO LENS

7   +3 DIOPTER SUPPLEMENTARY LENS

8   EXTENSION TUBE

9   PHOTOSONIC CAMERA

10 100-w MERCURY ARC POINT SOURCE

11 FRONT SURFACE MIRROR FOR VISIBLE LIGHT RECORDING

12 KNIFE EDGE

13 6-in. - SQUARE CORNING IR FILTER (7-56). REMOVES VISIBLE
    LIGHT FROM ARC SOURCE.

70718

Figure B-3. Simultaneous Visible and Schlieren
Photography of Arc Image Furnace

DOCUMENT CONTROL DATA · R&D

(Security classification of title, body of abstract and indexing annotation must be entered when the overall report is classified)

1. ORIGINATING ACTIVITY (Corporate author)	2a. REPORT SECURITY CLASSIFICATION
United Technology Center, Division of United Aircraft Corp, Chemical Physics Research Division Sunnyvale, California 94088	UNCLASSIFIED
	2b. GROUP

3. REPORT TITLE

COMPOSITE SOLID PROPELLANT IGNITION MECHANISMS

4. DESCRIPTIVE NOTES *(Type of report and inclusive dates)*

AFOSR Scientific Report — 1 April 1966 through 31 March 1967 (Interim)

5. AUTHOR(S) *(Last name, first name, initial)*

Shannon, Larry J.

6. REPORT DATE	7a. TOTAL NO. OF PAGES	7b. NO. OF REFS
September 1967	61	14

8a. CONTRACT OR GRANT NO.	9a. ORIGINATOR'S REPORT NUMBER(S)
AF 49(638)-1557	
b. PROJECT NO. 9711-01	UTC 2138-ASR2
c. 61445014	9b. OTHER REPORT NO(S) (Any other numbers that may be assigned this report)
d. 681308	AFOSR 67-1765

10. AVAILABILITY/LIMITATION NOTICES

Each transmittal of this document outside the agencies of the U.S. Government must have prior approval of AFOSR(SRGL).

11. SUPPLEMENTARY NOTES	12. SPONSORING MILITARY ACTIVITY
Tech, Other	Air Force Office of Scientific Research (SREP) 1400 Wilson Boulevard Arlington, Virginia 22209

13. ABSTRACT

This report describes the work performed under AFOSR Contract No. AF 49(638)-1557 during the period 1 April 1966 through 31 March 1967. Surface structures of thermoplastic and elastomeric fuels were found to be markedly different upon exposure to conductive heating from a doubly compressed stagnant gas at oxygen concentrations below those required to cause ignition. The thermoplastic polymer exhibited a molten surface, while the elastomeric fuels showed no visible changes. Vaporization followed by a gas-phase reaction is the probable ignition mechanism for the thermoplastic fuels in the shock tube environment. A gas-solid reaction may occur in the ignition of elastomeric polymers. No general conclusion can be drawn regarding the precise nature of the oxygen-polymer ignition process in the shock tube environment as consideration must be given to the physical structure of the polymer surface.

Ignition characteristics of several representative ammonium perchlorate composite propellants were studied using the arc-imaging furnace. The nature of the fuel component was found to have the major influence on the ignition time, and the effect is related to the initial pressure. A model describing composite propellant ignition in a neutral environment was formulated and programmed for computer studies.

DD FORM 1473 (1 JAN 64)

55

14. KEY WORDS	LINK A		LINK B		LINK C	
	ROLE	WT	ROLE	WT	ROLE	WT
Composite solid propellant						
Ignition						
Shock tube						
Arc-image furnace						
Experiments						
Theory						

INSTRUCTIONS

1. ORIGINATING ACTIVITY: Enter the name and address of the contractor, subcontractor, grantee, Department of Defense activity or other organization (corporate author) issuing the report.

2a. REPORT SECURITY CLASSIFICATION: Enter the overall security classification of the report. Indicate whether "Restricted Data" is included. Marking is to be in accordance with appropriate security regulations.

2b. GROUP: Automatic downgrading is specified in DoD Directive 5200.10 and Armed Forces Industrial Manual. Enter the group number. Also, when applicable, show that optional markings have been used for Group 3 and Group 4 as authorized.

3. REPORT TITLE: Enter the complete report title in all capital letters. Titles in all cases should be unclassified. If a meaningful title cannot be selected without classification, show title classification in all capitals in parenthesis immediately following the title.

4. DESCRIPTIVE NOTES: If appropriate, enter the type of report, e.g., interim, progress, summary, annual, or final. Give the inclusive dates when a specific reporting period is covered.

5. AUTHOR(S): Enter the name(s) of author(s) as shown on or in the report. Enter last name, first name, middle initial. If military, show rank and branch of service. The name of the principal author is an absolute minimum requirement.

6. REPORT DATE: Enter the date of the report as day, month, year; or month, year. If more than one date appears on the report, use date of publication.

7a. TOTAL NUMBER OF PAGES: The total page count should follow normal pagination procedures, i.e., enter the number of pages containing information.

7b. NUMBER OF REFERENCES: Enter the total number of references cited in the report.

8a. CONTRACT OR GRANT NUMBER: If appropriate, enter the applicable number of the contract or grant under which the report was written.

8b, 8c, & 8d. PROJECT NUMBER: Enter the appropriate military department identification, such as project number, subproject number, system numbers, task number, etc.

9a. ORIGINATOR'S REPORT NUMBER(S): Enter the official report number by which the document will be identified and controlled by the originating activity. This number must be unique to this report.

9b. OTHER REPORT NUMBER(S): If the report has been assigned any other report numbers (either by the originator or by the sponsor), also enter this number(s).

10. AVAILABILITY/LIMITATION NOTICES: Enter any limitations on further dissemination of the report, other than those imposed by security classification, using standard statements such as:

(1) "Qualified requesters may obtain copies of this report from DDC."

(2) "Foreign announcement and dissemination of this report by DDC is not authorized."

(3) "U. S. Government agencies may obtain copies of this report directly from DDC. Other qualified DDC users shall request through

_____ ."

(4) "U. S. military agencies may obtain copies of this report directly from DDC. Other qualified users shall request through

_____ ."

(5) "All distribution of this report is controlled. Qualified DDC users shall request through

_____ ."

If the report has been furnished to the Office of Technical Services, Department of Commerce, for sale to the public, indicate this fact and enter the price, if known.

11. SUPPLEMENTARY NOTES: Use for additional explanatory notes.

12. SPONSORING MILITARY ACTIVITY: Enter the name of the departmental project office or laboratory sponsoring (paying for) the research and development. Include address.

13. ABSTRACT: Enter an abstract giving a brief and factual summary of the document indicative of the report, even though it may also appear elsewhere in the body of the technical report. If additional space is required, a continuation sheet shall be attached.

It is highly desirable that the abstract of classified reports be unclassified. Each paragraph of the abstract shall end with an indication of the military security classification of the information in the paragraph, represented as (TS) (S), (C), or (U).

There is no limitation on the length of the abstract. However, the suggested length is from 150 to 225 words.

14. KEY WORDS: Key words are technically meaningful terms or short phrases that characterize a report and may be used as index entries for cataloging the report. Key words must be selected so that no security classification is required. Identifiers, such as equipment model designation, trade name, military project code name, geographic location, may be used as key words but will be followed by an indication of technical context. The assignment of links, rules, and weights is optional.

SUPPLEMENTARY

INFORMATION

NOTICE OF CHANGES IN CLASSIFICATION, DISTRIBUTION AND AVAILABILITY

69-18   15 SEPTEMBER 1969

AD-820 453L United Technology Center, Sunnyvale, Calif. Research and Advanced Technology Dept. Scientific rept. 1 Apr 66-31 Mar 67. Rept. no. UTC-2138-ASR-2, AFOSR-67-1765 Sep 67 Contract AF 49(638)-1557	USGO: others to Air Force Office of Scientific Research, Attn: SRGL, Arlington, Va.	No Foreign without approval of Air Force Office of Scientific Research, Attn: SRGL, Arlington, Va.	AFOSR notice, 15 Jul 69